



United States
Department of
Agriculture

Forest Service



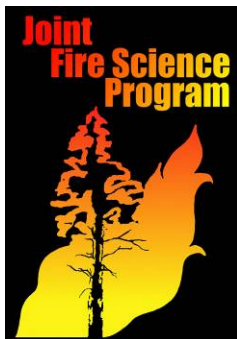
Pacific Northwest
Research Station

**Mapping and analysis of pre-fire fuels
loading and burn intensity using pre-fire
interferometric synthetic aperture radar data
combined with burn intensity derived from
post-fire multispectral imagery for the 2003
southern California fires**

**Final Report to the
Joint Fire Science Program
March 2009**

JFSP Project Number 04-1-2-02

Robert J. McGaughey
Andrew G. Cooke
Hans-Erik Andersen
Stephen E. Reutebuch



The Forest Service of the U.S. Department of Agriculture is dedicated to the principle of multiple use management of the Nation's forest resources for sustained yields of wood, water, forage, wildlife, and recreation. Through forestry research, cooperation with the States and private forest owners, and management of the National Forests and National Grasslands, it strives—as directed by Congress—to provide increasingly greater service to a growing Nation.

The U.S. Department of Agriculture (USDA) prohibits discrimination in all its programs and activities on the basis of race, color, national origin, gender, religion, age, disability, political beliefs, sexual orientation, or marital or family status. (Not all prohibited bases apply to all programs.) Persons with disabilities who require alternative means for communication of program information (Braille, large print, audiotape, etc.) should contact USDA's TARGET Center at (202) 720-2600 (voice and TDD).

To file a complaint of discrimination, write USDA, Director, Office of Civil Rights, Room 326- W, Whitten Building, 14th and Independence Avenue, SW, Washington, DC 20250-9410 or call (202) 720-5964 (voice and TDD). USDA is an equal opportunity provider and employer.

USDA is committed to making its information materials accessible to all USDA customers and employees.



Authors

Robert J. McGaughey, Hans-Erik Andersen, and Stephen E. Reutebuch are research foresters, U.S. Department of Agriculture, Forest Service, Pacific Northwest Research Station.

Table of Contents

Project Summary.....	1
Significant Findings.....	2
Management Implications.....	4
Deliverables.....	5
Introduction.....	6
Project Overview.....	6
Technology Overview.....	7
Study Sites and Data Resources.....	13
Remotely-Sensed Data.....	13
Field Data.....	21
Methods.....	25
Data Fusion and Direct Comparison of LIDAR, IFSAR, and Field-Measured Vegetation Heights.....	25
LIDAR-derived Bare-earth Surface Assessment.....	27
IFSAR P-band Bare-earth Surface Assessment.....	29
IFSAR X-band Vegetation Height Assessment.....	30
Results and Discussion.....	33
Direct Comparison of LIDAR, IFSAR, and Field-Measured Vegetation Heights.....	33
LIDAR-derived Bare-earth Surface Accuracy.....	36
IFSAR P-band Bare-earth Surface Accuracy.....	38
IFSAR X-band Vegetation Height Accuracy.....	39
Conclusions.....	44
Recommendations Regarding the Use of Ifsar Data for Vegetation Mapping.....	47
Acknowledgements.....	47
Literature Cited.....	48
Appendices.....	50
Appendix A -- Field Plot Measurement Protocol.....	51
Appendix B -- Outputs.....	60
Published Outputs.....	60
Presentations.....	61

Project Summary

SAR (Synthetic Aperture Radar) is an active sensing technology that emits and records the reflection of microwave radio energy. Interferometric SAR (IFSAR) uses the difference in phase, or phase shift, between two SAR images acquired from slightly different locations to determine the three-dimensional location of target objects. By varying the wavelength of the emitted energy, it is possible to measure different materials. Sensors emitting pulses with short wavelength (i.e. X-band IFSAR with $\lambda = 3$ cm) can measure the surface structure of the forest canopy, while sensors with longer wavelengths (P-band IFSAR with $\lambda = 72$ cm) create a surface corresponding to the ground. Today, there are only a few vendors that provide IFSAR data. The technology is still being proven. In general, the cost for acquiring IFSAR is about \$0.25/ha for large areas (40,000 ha and larger).

During 2002-2003, the National Oceanic and Atmospheric Administration, Coastal Services Center (NOAA) and the Southern California Wetland Recovery Project (SCWRP) contracted with EarthData International (EDI) to collect IFSAR data over coastal watersheds from Point Conception, CA to the US border with Mexico using their GeoSAR system. The data acquisition covered all of the areas burned by the 2003 southern California fires.

This project was designed to evaluate the utility of the high-resolution GeoSAR dataset for characterizing vegetation structure in the chaparral-dominated landscapes characteristic over much of southern California (SoCal). While the original project objectives included the development of pre-fire vegetation maps for several areas burned in 2003, we found that limitations with the P-band IFSAR acquisition and the inability to process the data to produce a ground surface model prevented large-area mapping. The project emphasis was shifted to focus on the accuracy of X-band IFSAR products and their use in conjunction with a ground-surface model (developed using other technologies) to map vegetation height and structure. The following specific objectives were addressed:

- Assess the utility of airborne X-band IFSAR for measurement of canopy height, when used in combination with a LIDAR-derived terrain model, in dry fire-prone forests within southern California and central Washington State.
- Assess the utility of airborne P-band IFSAR for measurement of terrain elevation under dense forest canopy in mixed-conifer forests of western Washington.
- Development and demonstration of field protocol to measure vegetation composition and structure in chaparral, mixed conifer, and oak woodland forest types within southern California.
- Assess the utility of airborne LIDAR to measure terrain elevations and vegetation heights within fire-prone chaparral ecosystems in southern California.

Significant Findings

IFSAR systems utilize a broad spectrum of radio frequencies. Unfortunately many of the frequencies used with the longer wavelength variant, P-band, conflict with those used for civilian and military communications systems. The Federal Communications Commission (FCC) imposes restrictions on specific frequencies and frequency ranges to ensure that IFSAR missions do not inter with radio communications. For the SoCal GeoSAR acquisition, the preprogrammed waveform was “notched” to assure that there was no interference with other users of these frequencies. In general, this “notching” reduces the accuracy of the P-band radar measurements and degrades the resulting P-band ground surface. For the NOAA SoCal acquisition, restrictions were so severe that EarthData could not process the P-band data to produce a useable ground surface making direct measurement of vegetation heights impossible. Unfortunately, similar restrictions on the frequency spectra are in effect for most areas in the continental U.S. severely limiting the usefulness of P-band data products. In another acquisition conducted in Columbia, South America, EarthData found that airborne P-band data collected without the frequency restrictions could be processed to provide a reasonable ground surface thus allowing direct measurement of vegetation height using only IFSAR-derived data. There are no similar restrictions on the frequencies used for X-band IFSAR.

In a related study using P-band IFSAR data acquired for a different study area without the frequency restrictions (permission was granted for the acquisition because of an administrative error in the application process), we found that the mean elevation difference between the IFSAR ground surface and the elevation of 347 checkpoints was -0.28 ± 2.59 m (mean \pm SD). The RMSE was 2.60 m. The overall terrain accuracy was not significantly affected by the density of the vegetation cover or the terrain slope. For comparison, we also evaluated standard USGS 10 m elevation models (DEM) using the same topographic checkpoints. The mean error of the USGS DEM was found to be 7.3 ± 4.9 m (mean \pm SD), with a maximum observed error of 18.07 m and a minimum of -4.91 m. The RMSE of the USGS DTM was 8.8 m. These results make it clear that P-band IFSAR can produce accurate ground surface models in the absence of the FCC restrictions.

While we found the IFSAR-derived ground surface models were inadequate for determining vegetation height, we found that X-band IFSAR can be used with a ground surface from a different source (LIDAR) to produce measurements of vegetation height. The accuracy of canopy height measurements obtained using this combination of remotely-sensed data is not significantly influenced by the flying height (above ground) for the X-band component. We found that the accuracy of the vegetation height measurements is influenced by the overall vegetation density. Areas covered by low-density vegetation (plants per unit area) generally have larger errors compared to areas with higher vegetation densities. IFSAR generally does not measure small (less than one tree height in diameter) gaps so the vegetation height is usually overestimated in low-density vegetation. For the most accurate height measurements, especially in mountainous terrain, data from multiple look angles should be combined to minimize

gaps in the data due to radar shadows (areas occluded due to topography and localized canopy features) and the influence of terrain slope.

In general, IFSAR underestimates vegetation height regardless of the vegetation density or type. When comparing field measurements to those computed using an IFSAR X-band vegetation surface and a LIDAR bare-earth surface, we found that the average vegetation height for a plot was $1.56 \text{ m} \pm 2.13 \text{ m}$ (mean \pm SD) less than the average of the heights measured in the field. In vegetation composed of a mixture of small trees (height $\leq 5\text{m}$) and shrubs, the error was smaller ($0.19 \pm 1.69 \text{ m}$). For areas with large trees (height $> 5 \text{ m}$), the error was larger ($1.99 \pm 3.46 \text{ m}$). In all vegetation types, the IFSAR surface appeared excessively “smoothed” and did not capture details at the individual tree/plant level.

Field measurement of vegetation in the dense chaparral and shrub types common in SoCal is difficult and time consuming. For this study, we developed and tested a field measurement protocol for use in dense chaparral, shrub, and mixed shrub/tree vegetation types (Appendix A). This protocol produces precisely geo-referenced data that can be compared to a variety of remotely-sensed information. We measured 35 plots over a variety of vegetation types and densities and found the protocol efficient and useful.

Because the IFSAR P-band data cannot be processed to produce accurate bare-earth ground surfaces, some other method must be used to provide this necessary component. We evaluated the accuracy of a LIDAR-derived bare-earth surface using 1,709 terrain points throughout the study areas used to compare field measurements to IFSAR canopy height measurements. Overall the LIDAR ground elevations were $0.04 \pm 0.61 \text{ m}$ (mean \pm SD) above the terrain point elevations. In the highest density vegetation, the LIDAR ground elevations were $0.10 \pm 0.69 \text{ m}$ above the terrain point elevations, and this increased to $0.13 \pm 0.70 \text{ m}$ in the tallest vegetation category.

Management Implications

Two types of remote sensing, LIDAR and IFSAR, are commercially available to produce three-dimensional measurements of vegetation, structures, and the ground surface. The use of LIDAR for producing accurate, high-resolution terrain models has become widespread. Its use for characterizing vegetation characteristics is much less developed. The cost to acquire LIDAR is about \$2.50/ha for projects larger than 40,000 ha and the resulting sample density is between 4 and 8 samples/m². IFSAR is less readily available with only two vendors operating in North America. The cost to acquire IFSAR is about \$0.25/ha for projects larger than 40,000 ha and the resulting sample density is less than 1 sample/m² (data are delivered in raster form using a 2-3 m cell size).

In a remote sensing context, two basic components are needed to directly characterize vegetation size and density: bare-ground surface elevations and canopy surface elevations. The bare-ground surface provides the point-of-reference needed to compute vegetation heights and to detect the presence or absence of vegetation. Without an accurate bare-ground surface, quantitative information related to plant size and overall vegetation density cannot be derived. Unfortunately, IFSAR alone cannot provide both of the necessary components.

In areas where an accurate bare-earth model is available (perhaps from a large-area LIDAR acquisition), vegetation height and the volume occupied by vegetation can be computed using the X-band IFSAR surface. Fortunately, the ground surface changes very little compared to the vegetation making it possible to use a bare-earth model produced years, or even decades prior to the acquisition of IFSAR data. Many state and local governments are currently obtaining LIDAR data to update their bare-earth surface layers and model flood risk. Such acquisitions produce accurate, high-resolution bare-earth surfaces that will be useful for years to come. Such acquisitions provide the baseline data for applications concerned with detecting change over large land areas. In this context, IFSAR can provide a cost effective, relatively high-resolution tool to obtain the raw measurements needed to monitor changes in vegetation characteristics.

Deliverables

See Appendix B for a complete list of published outputs and presentations.

Proposed	Delivered	Status
Pre-fire vegetation structure and fuels maps for three major fire areas	Cannot be completed	The pre-fire IFSAR data were determined to be unusable for this purpose due to data collection restrictions imposed by the FCC in the P-band frequency.
Evaluation of the utility of GeoSAR data for mapping vegetation structure and fuels	Completed	Peer-reviewed journal article published (Andersen, H.-E., R.J. McGaughey, and S.E. Reutebuch. 2008. Assessing the influence of flight parameters, interferometric processing, slope, and canopy density on the accuracy of X-band IFSAR-derived forest canopy height models. <i>International Journal of Remote Sensing</i> 29(5): 1495-1510); peer-reviewed book chapter published (Andersen, H.-E., S.E. Reutebuch, and R.J. McGaughey. 2006. Chapter 3: Active remote sensing. In: Shao, G., and K. Reynolds, eds., <i>Computer Applications in Sustainable Forest Management</i> , Springer-Verlag, Dordrecht, The Netherlands. p. 43-66.).
Recommendations for future use of existing GeoSAR dataset	Completed	See recommendations in report text.
Methodology for processing IFSAR data for vegetation structure mapping	Completed	Processing methods were included in published articles.
Visualization software for exploring and displaying 3-D IFSAR datasets	Completed	FUSION LIDAR processing and analysis software modifications to allow display and use of IFSAR surfaces, conversion of IFSAR surface data to point clouds, processing surface data to produce surface roughness metrics and volume between two surfaces (i.e., bare ground and vegetation). Available on the web at http://forsys.cfr.washington.edu/fusion.html
	Additional deliverable	Assessment of LIDAR-derived bare-ground surface accuracy in chaparral. MS Thesis: Andrew Cooke, University of Washington Complete

Introduction

We live in an information-rich age. Technologies such as geographic information systems (GIS) and Google Earth® allow us to integrate and interpret large volumes of spatial and temporal data on our desktops. We can literally view our environment from perspectives never before possible. With a few click of our mouse we can venture from high altitude views of our planet to our countries, cities, neighborhoods, and even our front doors. Databases are constantly being updated with more detailed information describing all facets of our existence. However, as alluring as the technology has become we still must rely on quantitative information to help us make informed decisions. In the forest management context, we do not have any methods available that produce quantitative descriptions of vegetation characteristics over large land areas in a rapid, cost effective manner.

This project titled “Mapping and analysis of pre-fire fuels loading and burn intensity using pre-fire interferometric synthetic aperture radar data combined with burn intensity derived from post-fire multispectral imagery for the 2003 southern California fires” investigates the potential application of Interferometric Synthetic Aperture RADAR (IFSAR) to map vegetation and fuel characteristics over large land areas.

Project Overview

In many parts of the West, there is severe fire danger as a result of high fuel loadings. Nowhere was this more evident in the 2003 fire season than in Southern California (SoCal), where over 650,000 acres burned in October in five counties (Ventura, Los Angeles, San Bernardino, Riverside, and San Diego). Reduction of fuels, particularly in wildland-urban-interface (WUI) areas is a national priority for the USDA Forest Service. The Healthy Forests Restoration Act of 2003 was signed into law to help speed the reduction of dangerous fuel loadings, with priority given to WUI areas. However, to better guide this effort, improved methods are needed to measure and map vegetation structure and associated fuel loadings. Additionally, improved methods for measuring fuel loading over landscapes are needed to build and validate fire behavior models. The emergence of a new generation of high-resolution remote sensing systems could potentially allow for more accurate and efficient estimation of fuels and fire behavior variables. With spatial resolutions in the sub-meter range, the spatial data provided by these sensors can support more detailed measurement of vegetation structure. The ability of active microwave (radar) airborne sensors to penetrate the canopy may significantly improve estimation of the quantity and distribution of vegetation structure, moisture regimes, and density.

The original objectives of this project were to use the extensive existing pre-fire and post-fire datasets to:

- Evaluate the utility of the existing high-resolution GeoSAR (an X-band/P-band IFSAR system owned by EarthData International) dataset for vegetation structure mapping by developing high-resolution (1-3m range) pre-fire vegetation structure maps for 3 major 2003 SoCal fires,

- Compare GeoSAR-derived vegetation structure maps with BAER post-fire burn assessment maps to determine if pre-fire IFSAR vegetation measurements correlate well with fire intensity
- Make recommendations, in consultation with CDF, regarding the desirability of using the existing GeoSAR dataset to improve fuels maps in SoCal.

Problems with the primary GeoSAR dataset, namely the lack of a P-band-derived ground surface layer, forced reevaluation of these objectives. Previous studies (JFSP Project 01-1-4-07 and other non-JFSP-funded projects) demonstrated the utility of IFSAR for characterizing above ground biomass and canopy fuels (Andersen et al. 2008, Andersen et al. 2005). However, these initial investigations into IFSAR's ability to characterize vegetation relied on an X-/P-band airborne IFSAR dataset that was collected without the frequency limitations required by the Federal Communications Commission (FCC). These limitations, primarily affecting the P-band data, make it impossible to derive an accurate ground surface layer in vegetated areas. Without such a P-band derived ground surface layer, information captured by the X-band data cannot be used to independently compute vegetation heights and volumes. During the early stages of this project (mainly work done in 2004), we consulted with EarthData International's principal scientist to determine whether or not it was possible to process the P-band data to produce any useable information. EarthData was processing a test area for the original client (NOAA) and the Southern California Wetland Recovery Project, using the P-band data to determine the best methods for processing the data and the quality of the ground surface derived from the data. Unfortunately this test revealed that the information derived from the P-band data was poor and did not provide a useable ground surface layer. In light of these problems with the primary data for this project, we formulated the following new objectives to better evaluate the utility of IFSAR data for characterizing vegetation attributes:

- Assess the utility of airborne X-band IFSAR for measurement of canopy height, when used in combination with a lidar-derived terrain model, in dry fire-prone forests within southern California and central Washington State.
- Assess the utility of airborne P-band IFSAR for measurement of terrain elevation under dense forest canopy in mixed-conifer forests of western Washington.
- Development and demonstration of field protocol to measure vegetation composition and structure in chaparral, mixed conifer, and oak woodland forest types within southern California.
- Assess the utility of airborne lidar to measure terrain elevations and vegetation heights within fire-prone chaparral ecosystems in southern California.

Technology Overview

Two relatively new remote-sensing technologies were used for this project: Interferometric Synthetic Aperture RADAR (IFSAR) and Light Detection and Ranging (LIDAR). Both technologies produce three-dimensional measurements encompassing large land areas and include information relevant to the study of both ground surface and vegetation characteristics.

IFSAR

SAR (Synthetic Aperture Radar) is an active sensing technology that emits and records the reflection of microwave radio energy. The information content of radar data in forested terrain varies depending upon the wavelength (λ) of the transmitted pulses – energy with short wavelengths ($\lambda \sim 1$ cm) is reflected from the canopy surface while radar energy with longer wavelengths ($\lambda \sim 1$ m) penetrates the foliage in the canopy and reflects from tree trunks and the terrain surface. Another characteristic of microwave remote sensing, in contrast to optical remote sensing, is the capability to penetrate cloud and smoke cover. The resulting image represents the intensity of the radar backscatter throughout the illuminated region. Because the reflection of the radar signal is dependent upon the dielectric properties of the scattering elements within the resolution cell, SAR can also be used to measure soil moisture and canopy water content. While previous studies have shown that SAR backscatter amplitude data can be used to estimate forest biomass (Hussin et al., 1991), it has been noted that the biomass saturation limits for even long-wavelength SAR systems (~ 150 tons/ha) are too low to reach levels present in temperate closed forests (~ 300 tons/ha) (Mette et al., 2003).

The availability of high-resolution three-dimensional interferometric radar (IFSAR) data in recent years has the potential to significantly expand the applicability of radar analysis for forest structure analysis. Radar interferometry uses the difference in phase, or phase shift, between two radar images acquired from slightly different locations to acquire information relating to the elevation angle to an imaged point, which is used in conjunction with the range information to determine the three-dimensional location of this imaged point (Hagberg et al, 1995). Varying the wavelength of the emitted energy will allow collection of different three-dimensional structure data – sensors emitting pulses with short wavelength (i.e. X-band IFSAR with $\lambda = 3$ cm) can measure the surface structure of the forest canopy, while sensors with longer wavelengths (P-band IFSAR with $\lambda = 72$ cm) will generate a surface corresponding to the terrain elevation (Figure 1) Hofmann et al, 1999; Schwäbisch and Moreira, 1999). Accuracies of these systems also vary with wavelength; X-band interferometric radar data can have a vertical accuracy of 1-2 m, while P-band data has a vertical accuracy of 3-5 m (for GeoSAR system).

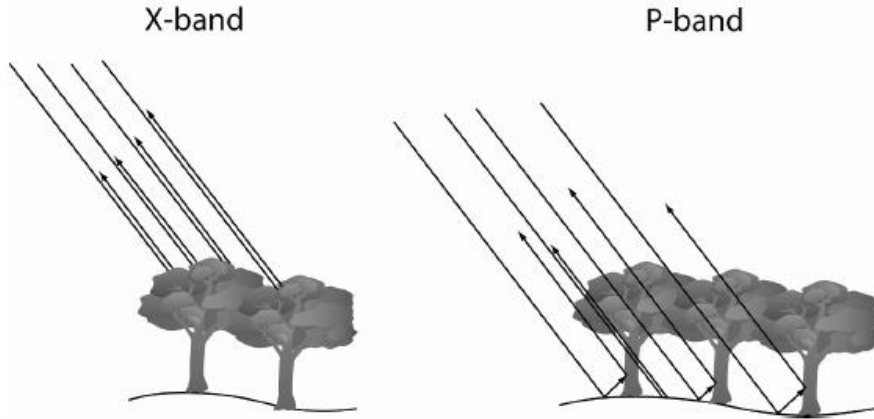


**Figure 1. Short wavelength X-band RADAR energy reflects from canopy surface while long wavelength P-band energy penetrates through canopy and reflects from stems and terrain surface
Adapted from Moreira et al. (2001).**

Past research has shown that polarimetric interferometric radar (PolInSAR) data acquired from single-frequency systems with wavelengths in the intermediate range (C- and L-band) can be used to extract information relating to the depth of various vegetation layers, the density of the scattering medium (related to biomass), and the elevation of the terrain surface (Treuhaft et al, 1996; Cloude and Papathanassiou, 1998). While many of these studies assumed an (admittedly simplistic) homogeneous density for the vegetation layer to reduce the number of parameters in the model, they have established the theoretical basis for more complex, and realistic, inferential approaches to the estimation of canopy density characteristics from IFSAR data. These authors have also noted that accuracy in the estimation of vegetation density and canopy characteristics would be expected to improve significantly through the analysis of multifrequency IFSAR data.

The GeoSAR multi-frequency IFSAR (X- and P-band) system operated by EarthData International (now part of Fugro) can provide canopy- and terrain-level elevation models as standard deliverable products. The GeoSAR system is a multifrequency IFSAR system mounted on a Gulfstream II jet operating from a flying altitude of 15,000 – 30,000 feet which acquires both X-band and P-band data in a single-pass mode at a rate of 8,800 km² per hour (see Figure 2). System parameters for the GeoSAR system are given in Table 1.

Table 1. GeoSAR system parameters.

Parameter	X-band	P-band
Center frequency	9.755 GHz	350 MHz
Wavelength	3 cm	86 cm
Bandwidth	80/160 MHz	80/160 MHz
Peak transmit power	8 kW	4 kW
Polarization	VV	HH, HV
Swath width	20 km	20 km

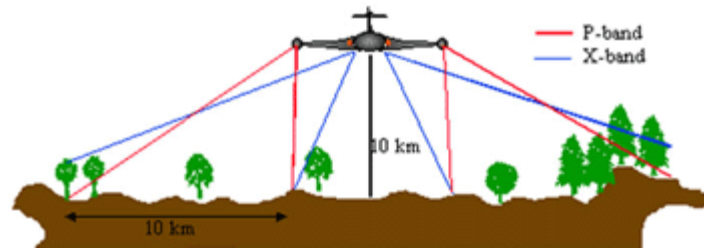


Figure 2. GeoSAR multifrequency IFSAR system.

The flight path is configured such that each point on the ground is imaged four times, from four different look angles. Co-polarized (HH, or horizontal transmit – horizontal receive) and cross-polarization (HV, or horizontal transmit-vertical receive) information is available at the P-band, while X-band data are acquired in co-polarized (VV) mode.

The difference of the canopy elevation (X-band) and underlying terrain elevation (P-band) yields a canopy height model that represents a spatially-explicit description of canopy structure (i.e. volume, height, biomass, etc.) over a given area of forest. The use of multi-frequency (X-band and P-band) IFSAR systems for forest mapping has emerged relatively recently, where research efforts have largely focused on improving forest type classification (Hofmann et al., 1999; Dutra et al. 2002; Mura et al., 2001).

LIDAR

Airborne laser scanning, also known by the acronym LIDAR (Light Detection and Ranging), is an operationally mature remote sensing technology that can provide highly-accurate measurements of both forest canopy and ground surface¹. A LIDAR sensor system essentially works upon the principle of measuring the time interval between the emission and reception of laser pulses. Range measurement is performed by multiplying this time interval by the speed of light ($R = c \times t/2$ (where, R is the range, t is the time interval between emission and receiving the pulse, and c is the speed of light, a known constant: 3×10^8 m/s)). The leading edge of the returning signal is not a well-defined point, so the time is usually recorded for a point at which the signal exceeds a certain threshold level, which is usually defined as a constant fraction of the signal peak (Baltsavias 1999). If the precise orientation and position of the laser is known from an inertial measurement unit and airborne differential GPS systems, respectively, the 3D vector corresponding to each laser pulse can be reconstructed, and a 3D coordinate assigned to each reflection. The “raw” LIDAR data are then typically provided as an ASCII or binary file containing XYZ values corresponding to the coordinates of each laser reflection.

The power received by the sensor will depend upon target characteristics, including the physical properties of the target (i.e. diffuse vs. specular reflector) and absolute target, reflectivity. LIDAR systems used for topographic mapping applications usually operate in the near infrared range of the electromagnetic spectrum (800-1100 nm). While specifications vary among systems, current LIDAR systems emit from 5,000-200,000 pulses per second, and vary the scan angle using optical-mechanical devices such as oscillating mirrors. Most systems have the capability of recording multiple reflections

from a single laser pulse (i.e. up to 5 per pulse). For example, in a forest area a given pulse may reflect from branches or leaves within the vegetation canopy and the ground below (Figure 3). As the scan angle is usually limited to 15-20 degrees off nadir, this system acquires measurements along a “swath” beneath the aircraft (Figure 4). For airborne, small-footprint systems, the footprint, or spot size, of the LIDAR pulse when it reaches the ground (or canopy surface) ranges from 0.10-1 meter depending upon flying height. In forested areas, the energy from individual LIDAR pulses can penetrate through gaps, and can therefore provide measurements of the underlying terrain surface as well as the vegetation and man-made structures.

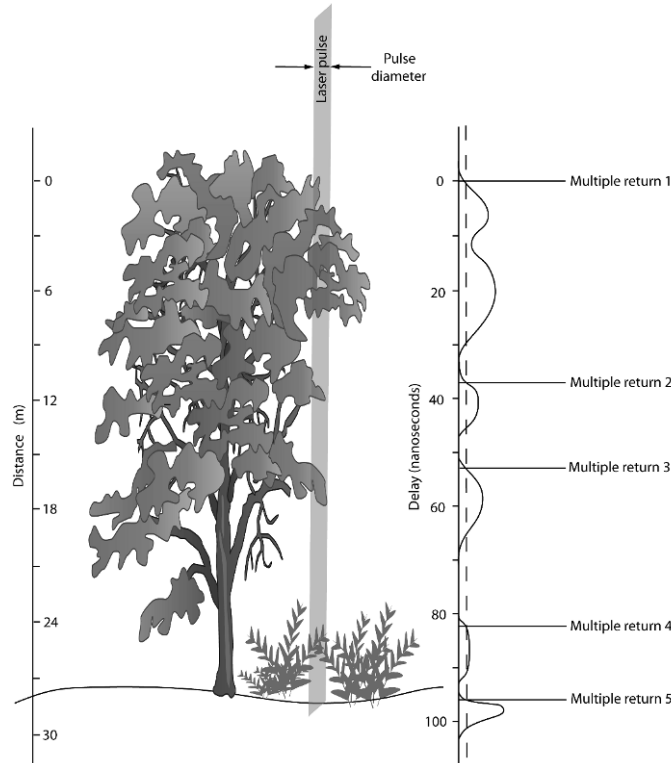


Figure 3. LIDAR remote sensing of vegetation. As the laser pulse passes through tree canopy, a signal is returned to the sensor. The leading edges of peaks in the returned signal correspond to multiple returns. Adapted from Lefsky et al. (2002).

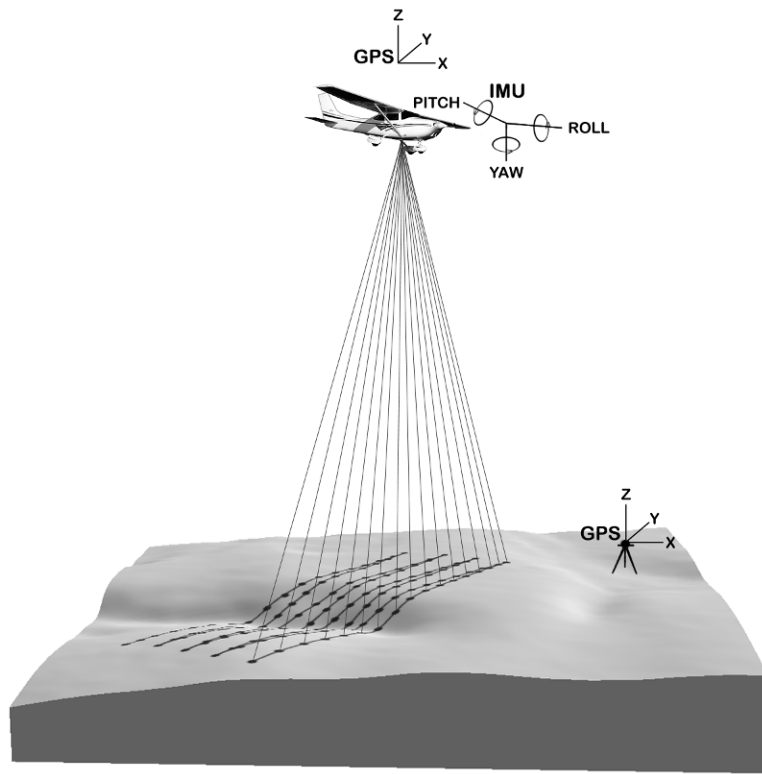


Figure 4. A schematic representation of airborne laser scanning.

Study Sites and Data Resources

Remotely-Sensed Data

A variety of remotely-sensed data were used for this project. Some of the data were collected before the 2003 fires and some after. Only the subset of the available data for the study sites actually used for analyses are described. Additional data were available from the California Department of Forestry and Fire Protection (CDF) and the Burn Area Emergency Response (BAER) team, namely fire fuels maps derived from LANDSAT imagery and FIA plot data, maps of vegetation mortality, and soil burn severity. These data were to be compared to a new vegetation/fuels and burn severity map. However, because the GeoSAR data did not provide an adequate ground surface, we were unable to produce area-wide maps for such comparisons.

Pre-Fire IFSAR

During 2002-2003, the National Oceanic and Atmospheric Administration, Coastal Services Center (NOAA) and the Southern California Wetland Recovery Project (SCWRP) contracted with EarthData International (EDI) to collect interferometric synthetic aperture (IFSAR) data over coastal watersheds from Point Conception to the US border with Mexico using their GeoSAR system (Figure 5), which includes coverage of all the major fires in SoCal in 2003 in pre-burn condition. SCWRP intended to use this IFSAR dataset to develop GIS-based tools for prioritizing wetland restoration and conservation options. Analyses of riparian areas are being done across the region to identify areas with high ecological value and to examine the costs and benefits of using land-use and land-cover data collected at different spatial scales to map riparian vegetation. The project is also developing conceptual models that examine the habitat, hydrology, and biogeochemistry functions of wetlands within their landscape context. The SCWRP is a multi-agency effort within California and is led by the California Coastal Conservancy. Although the dataset was collected for analyses of riparian and wetland conditions, it covered the entire landscape and provided a unique opportunity to collaborate with SCWRP to develop region-wide approaches for high-resolution vegetation structure maps.

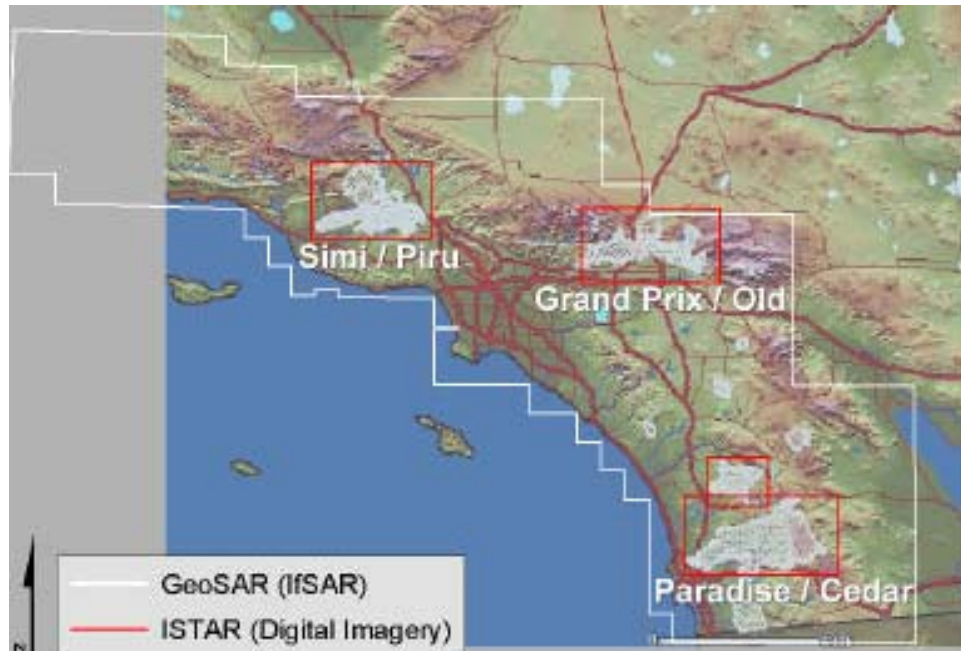


Figure 5. Extent of IFSAR data coverage (white outline) and ISTAR imagery, orthophotos, and DEMS (red outlines) available for proposed vegetation mapping.

In operation, GeoSAR's P-band RADAR uses a waveform consisting of frequencies ranging from 270 to 430 MHz. Unfortunately this range of frequencies is also used for civilian and military radio communication. The Federal Communications Commission (FCC) imposes restrictions on specific frequencies and frequency ranges to ensure that RADAR missions do not result in interference with radio communications. Figure 6 shows the X-band waveform with no frequency restrictions and Figure 7 shows the P-band waveform transmitted during the NOAA SoCal acquisition. For the SoCal GeoSAR acquisition, the preprogrammed waveform was "notched" to assure that there was no interference with other users of these frequencies. In general, this "notching" reduces the accuracy of the P-band radar measurements and degrades the resulting P-band ground surface. For the NOAA SoCal acquisition, restrictions were so severe that EarthData could not process the P-band data to produce a useable ground surface.

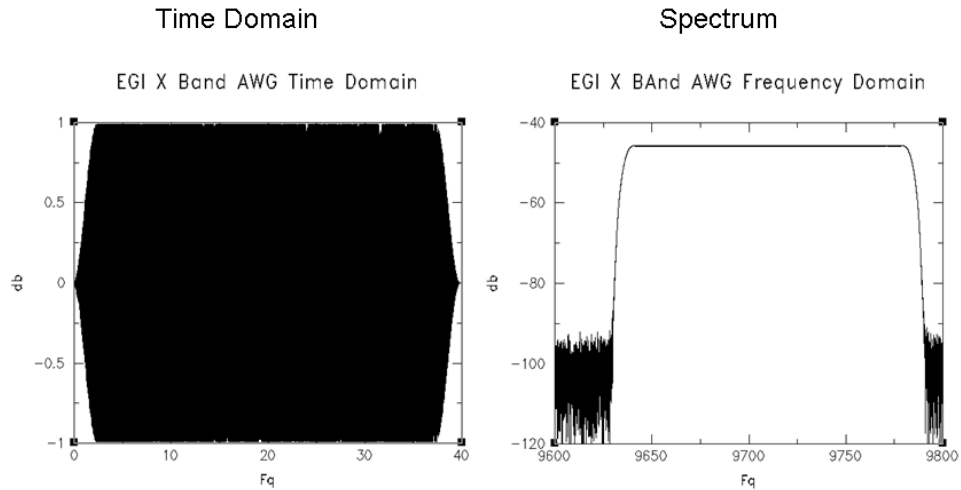


Figure 6. X-band waveform with no frequency restrictions.

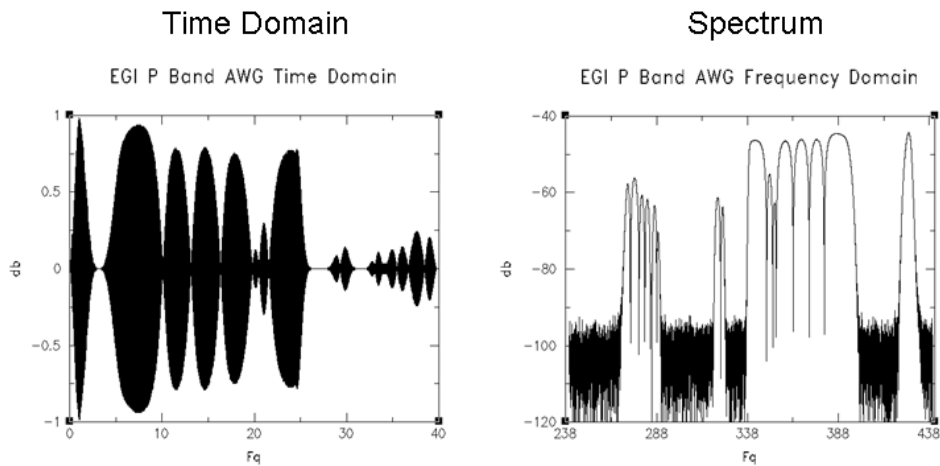


Figure 7. P-band waveform with all restricted frequencies removed ("notched"). Images courtesy of Brian Mercer.

The DEMs derived from the X-band IFSAR data are 3 m resolution and, for the most part, represent the top of the vegetation cover. Of course, in areas devoid of vegetation, the models represent the ground surface. Figure 8 shows an example DEM shaded to highlight topographic features.

The entire IFSAR dataset was available for this project. However, detailed analyses focused on three major burn areas: the Piru, Grand Prix, and Old fires.

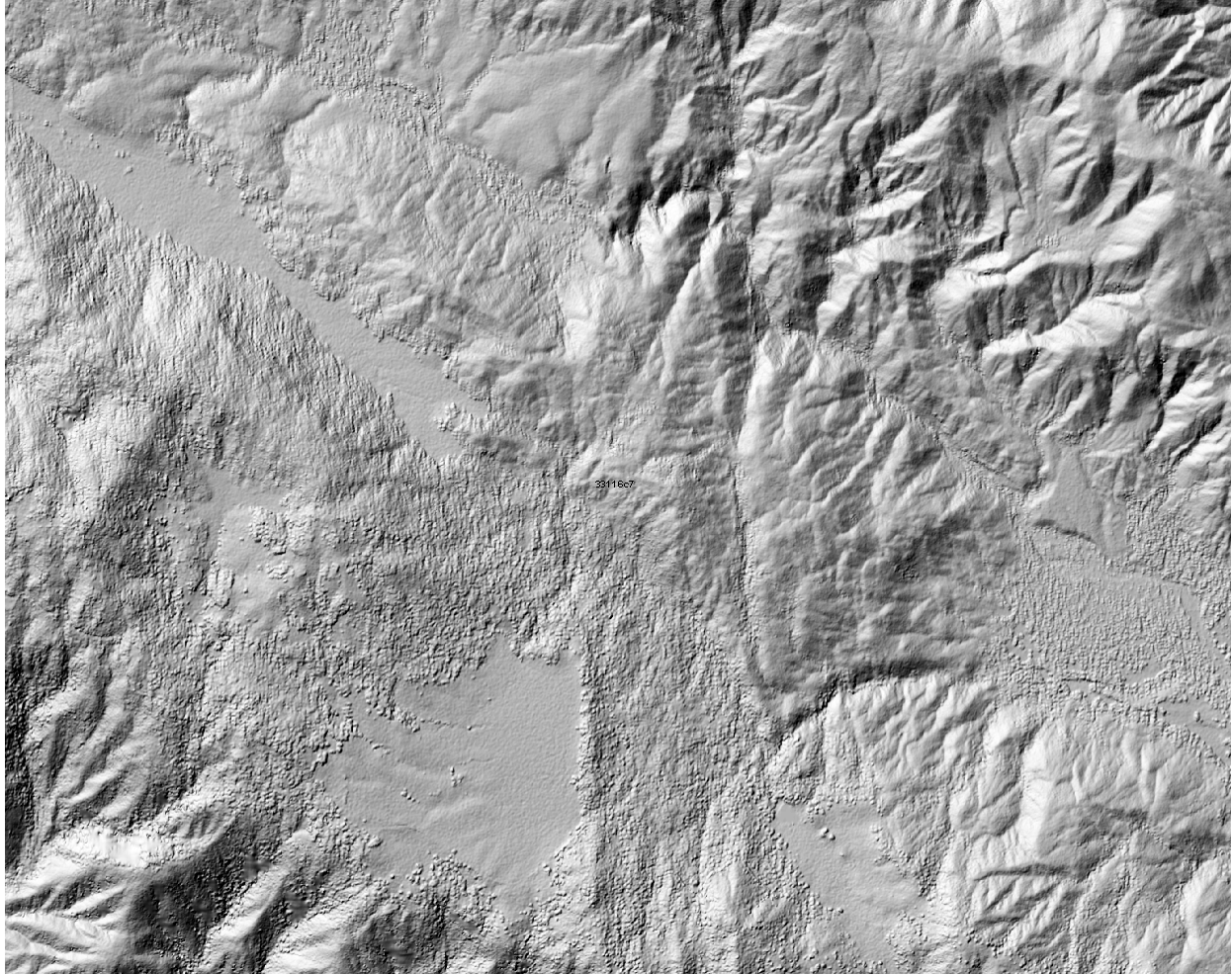


Figure 8. Example shaded surface rendering of X-band IFSAR-derived DEM. Rough areas are where the surface is on top of vegetation. In general, areas that appear smooth have no vegetation.

Post-Fire ISTAR Imagery

Immediately following the 2003 SoCal fires, EDI was also contracted to collect high-resolution, false-color digital infrared imagery (0.5 m resolution) over the major fires (Figure 5). This imagery was evaluated for use in this study. A sample image from the northern edge of the Old fire complex is shown in Figure 9. Products derived from the imagery included post-fire orthophotography and digital elevation models (DEMs) of unprecedented resolution and accuracy (3 m and 2 m resolution respectively). DEMs were produced from the imagery using photogrammetric autocorrelation techniques. As a result, the surface tends to represent the objects that can be easily matched in the images. For most areas within our study area, the final DEMs represent the top of the vegetation. Only in areas devoid of vegetation, for example within the burn perimeter, does the surface represent the ground.

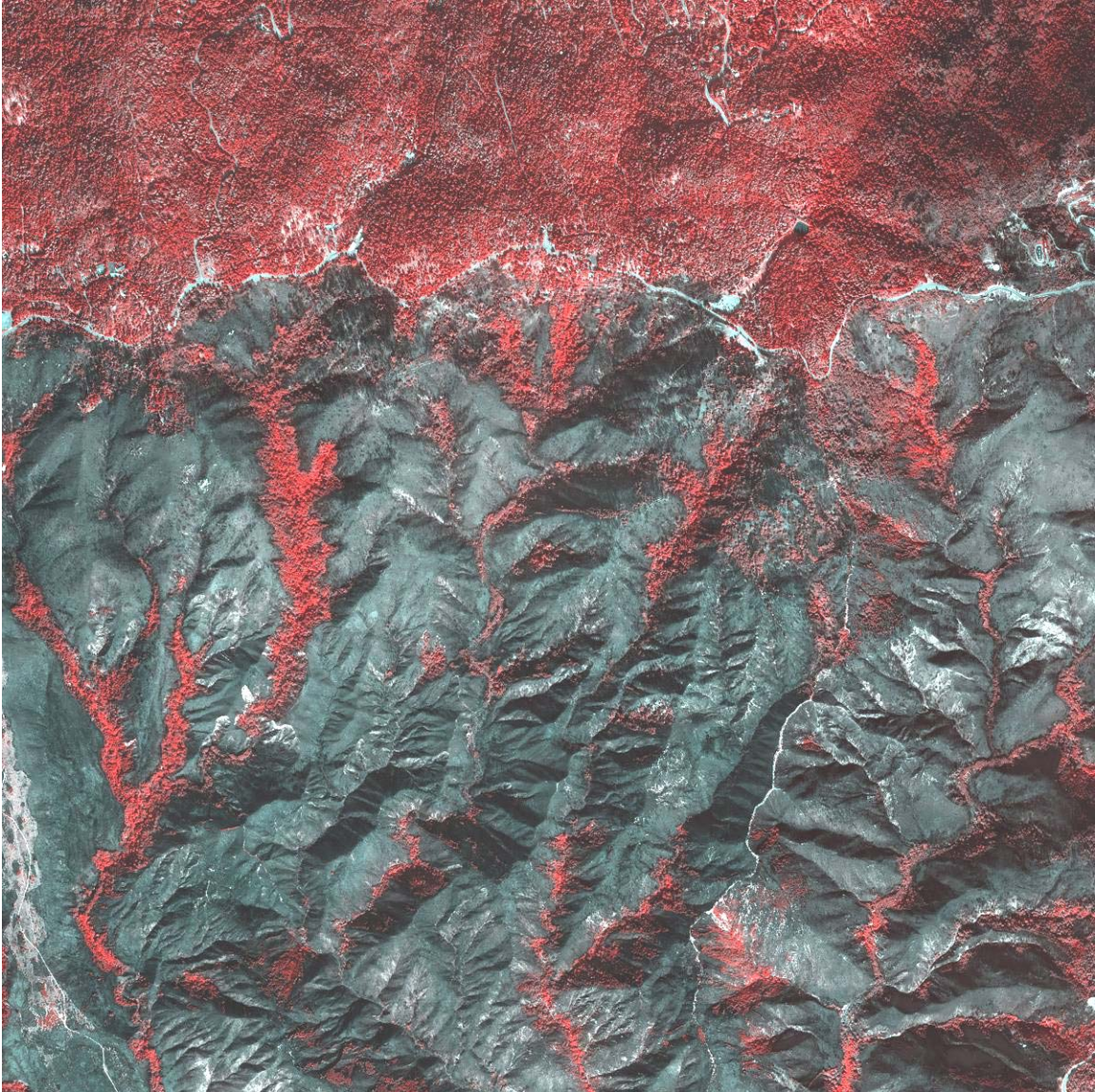


Figure 9. Sample ISTAR false-color infrared image from the northern edge of the old fire complex. The dark area in the lower two-thirds of the image is within the fire perimeter. Red areas contain live vegetation.

Comparing the ISTAR and IFSAR data products illustrates some of the problems with the bare-earth surfaces derived from these data. Figure 10 shows an ISTAR false-color infrared image. The most dominant feature in the image is the large “R”. This “landscape monogram” was created when the vegetation from areas within the letter was cut. As a result, the area within the “R” should be bare ground. Figure 11 shows the DEM derived from the ISTAR imagery. Notice that the “R” is embossed into the surface indicating the surface in the area surrounding the “R” is actually on top of the vegetation. The influence of the vegetation on the ISTAR-derived surface is further evident in the channels marked with the green and pink ovals. The image shows scattered vegetation with some bare areas. The DEM surface in this area shows characteristics of excessive smoothness. Most likely this is the result of poor image auto-correlation where only a few matching points were established. Gaps in the resulting

surface were filled by interpolating from adjacent areas. The net result is a surface that falls somewhere between the vegetation tops and the ground. In addition, the edges of the burn area are evident in the ISTAR surface (Figure 11) providing further evidence that the surface is being influenced by the presence or absence of vegetative cover. Comparing the IFSAR-derived surface, Figure 12, there is still evidence of the “R”. The drainages highlighted in the green and pink ovals have better definition but still have some surface roughness due to the sparse, but relatively large, vegetation.

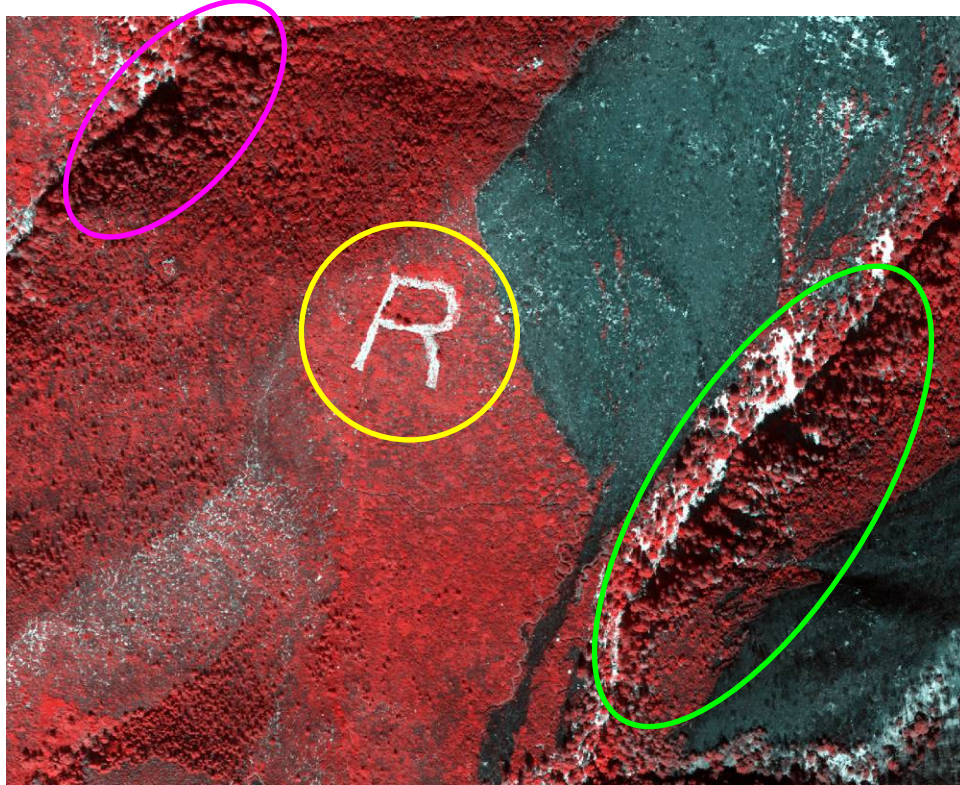


Figure 10. ISTAR false-color infrared image.

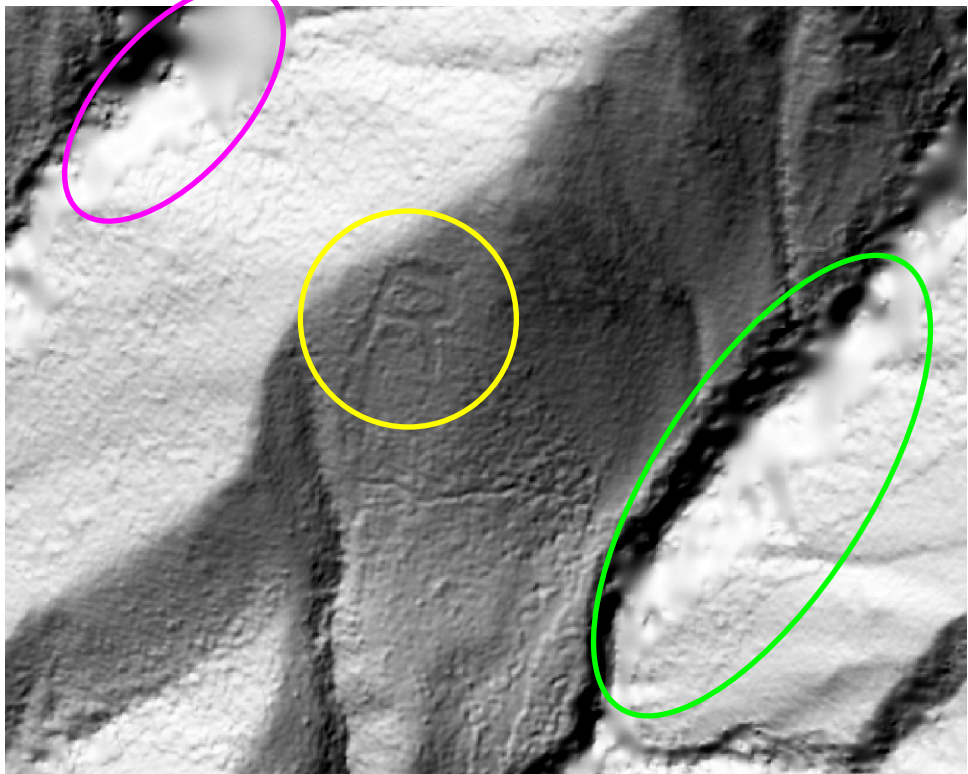


Figure 11. ISTAR-derived bare-earth surface.

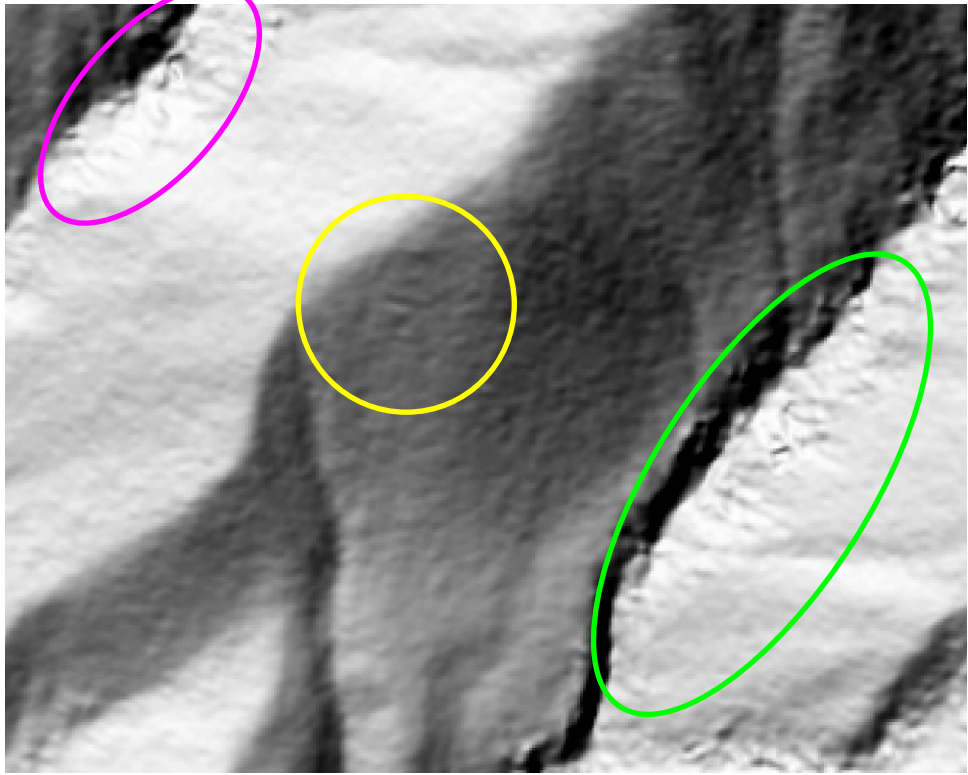


Figure 12. IFSAR-derived bare-earth surface. This surface was created from pre-fire data.

LIDAR

To establish high-quality bare ground surface models, LIDAR data were acquired for all field study sites. The LIDAR acquisition was divided into 5 separate collection areas. Two of the areas (PIRU1 and PIRU2) are located at the northern end of Piru lake (NE of Piru, CA). One area (GP1) is located SW of Cajon Junction, CA. The remaining two areas (OLD1 and OLD2) are located near Fredalba, CA. All areas are located in rugged terrain with elevations ranging from 100m to 1000m. The PIRU units, while located in somewhat moderate terrain are adjacent to the Sespe Condor Refuge which is characterized by rugged topography. Figure 13 shows the location of the PIRU1 and PIRU2 areas. Figure 14 shows the location of the GP1, OLD1, and OLD2 areas.

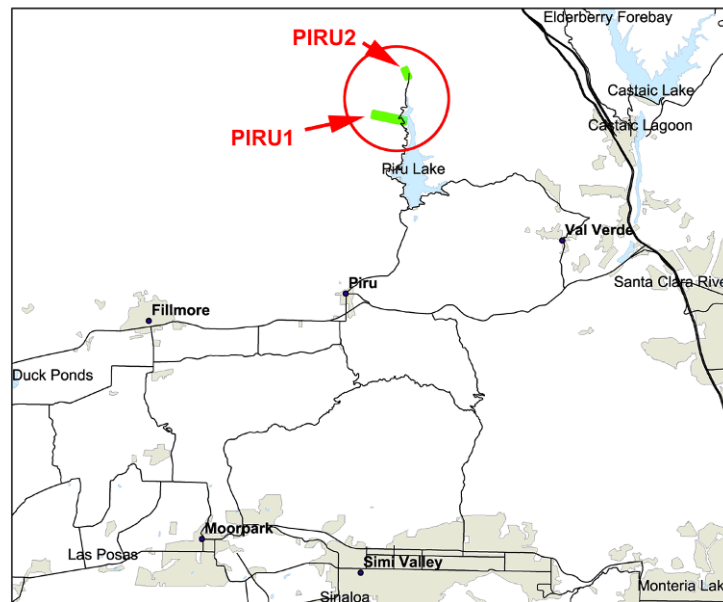


Figure 13. Location of PIRU1 and PIRU2 LIDAR acquisition areas.

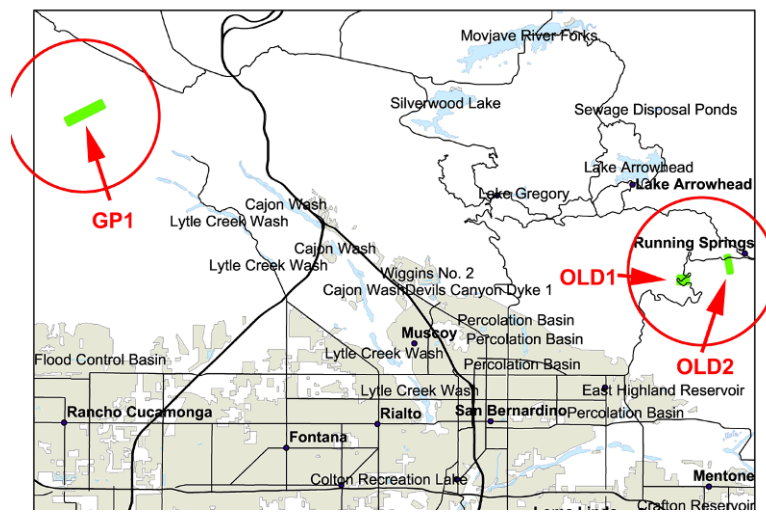


Figure 14. Location of the GP1, OLD1, and OLD2 LIDAR acquisition areas.

LIDAR data for the field sites were acquired on August 17, 2005. The data were collected using an Optech ALTM 3100 LiDAR system set to acquire four return laser points at an average spacing of less than 0.4 meters (greater than 4 points per square meter without overlap) for parallel 50% (nadir to side) overlapping areas. The scan angle was set to 9° from nadir to provide maximum penetration through the dense vegetation present over much of the acquisition area. The system recorded up to four individual laser point returns and the associated intensity for each laser echo. Table 2 summarizes the flight parameters. High-resolution (18-cm pixel) digital color imagery was simultaneously collected during the LIDAR acquisition.

Table 2. LIDAR flight parameters.

Scan Angle	18° (9° from Nadir)
Flight Above Ground Level (AGL)	1,000 m (terrain following)
Scan Pulse Repetition Frequency (PRF)	71 kHz (71,000 pulses per second)
Scan Width	~316 m
Flight Line Overlap	~100% (50% side-lap)
Over Land Data Density	>4 Points per square meter

Field Data

Vegetation heights were sampled during the summer of 2004 (19 plots) and 2005 (18 plots) using a 1/25-ha square plot with either 121 (2 m spacing) or 36 (4 m spacing) sample points distributed evenly over the plot. Appendix A describes the measurement protocol in detail. The sample point spacing was determined by the overall vegetation type and height. When the majority of the vegetation on the plot was less than 2m tall, the 2-meter spacing was used. Figure 15 shows a diagram of the plot design. The following information was recorded for each sample point:

- Maximum vegetation height (meters to the nearest 0.1m),
- Height to the base of the foliage layer,
- Dominant species at the point,
- Other species at the point,
- Indicator of whether or not vegetation was present at 0.5m height intervals from the ground to the maximum vegetation height. When the 4-meter grid was used, the height interval was 1.0 m.

For plots containing scattered, individual trees, additional data describing the trees were collected. Individual stem locations and the location of the horizontal center of the tree crown were surveyed. For each tree, species, diameter at breast height, height, crown width along an E-W and a N-S line, crown class (dominant, co-dominant, intermediate, suppressed), and a crown shape code were recorded. For plots dominated by tree cover, vegetation height and structure were measured using the sample points (usually spaced at 4 m).

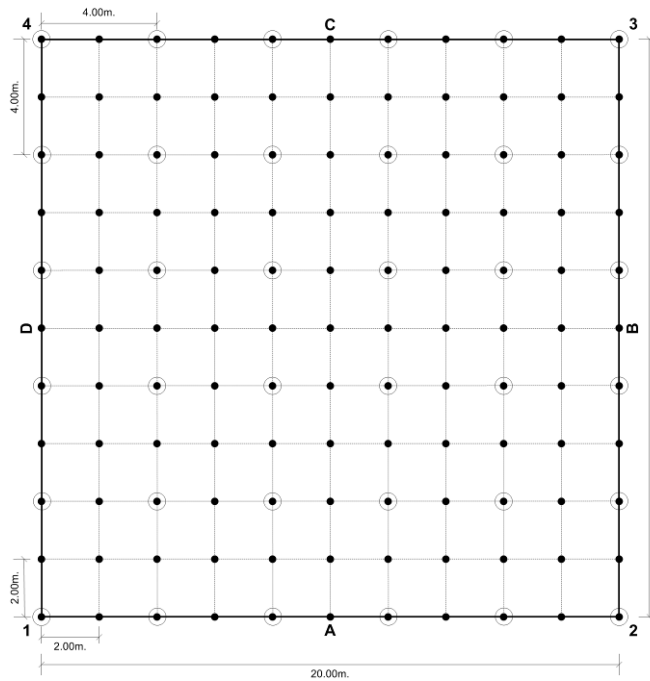


Figure 15. Schematic of the vegetation plot and measurement points.

The location of the vegetation plots measured in 2004 were obtained using differentially corrected GPS position data collected using a Trimble Pro XL GPS receiver. Plot locations measured in 2005 were obtained using JAVAD Maxor GPS receivers. All locations are generally accurate to within 1 meter (Clarkin, 2007)

To produce accurate position data using the Trimble GPS receivers, a network of three control points was established in the field for each measurement plot. Position data were collected for at least 500 epochs for each control point. Fore- and back-sightings from each control point to the other two were used along with a least-squares correction process to solve for the best combination of positions for the control points. This correction process relied on the computationally rigid geometry provided by the triangular arrangement of the three control points. Plot corners and tree locations were then surveyed from one or more of the control points.

The JAVAD receivers, used in 2005, provide sub-meter positions when used in open or sparse canopy areas so we simply positioned the units on each of the plot corners and recorded positions for about 15 minutes. No individual tree locations were mapped for the 2005 plots so no surveying was required.

Shrub plots were located within areas of homogeneous vegetation conditions (density and height) and uniform terrain conditions. Study areas were selected adjacent to areas burned during the 2003 fire season and within the IFSAR data coverage area. Plot locations were not randomized and did not include more than one vegetation/structure type. Figure 16 shows vegetation conditions typical on the Grand Prix and Old fire complex sites and Figure 17 shows conditions at the Piru complex site. Plots were established in the field by locating one corner of the plot and then, using 20-m long lines

marked at 2-m intervals and a compass, the other corners were established. Lines were hung around the plot perimeter and used to locate the sample points within the plot. Vegetation heights were measured with either a 2- or 3-m pole marked in 10-cm increments or a telescoping height pole (8 meter maximum height) with an analog display showing the height from the base of the pole to the top. Figure 18 shows the interior of a plot with the measurement lines in place.

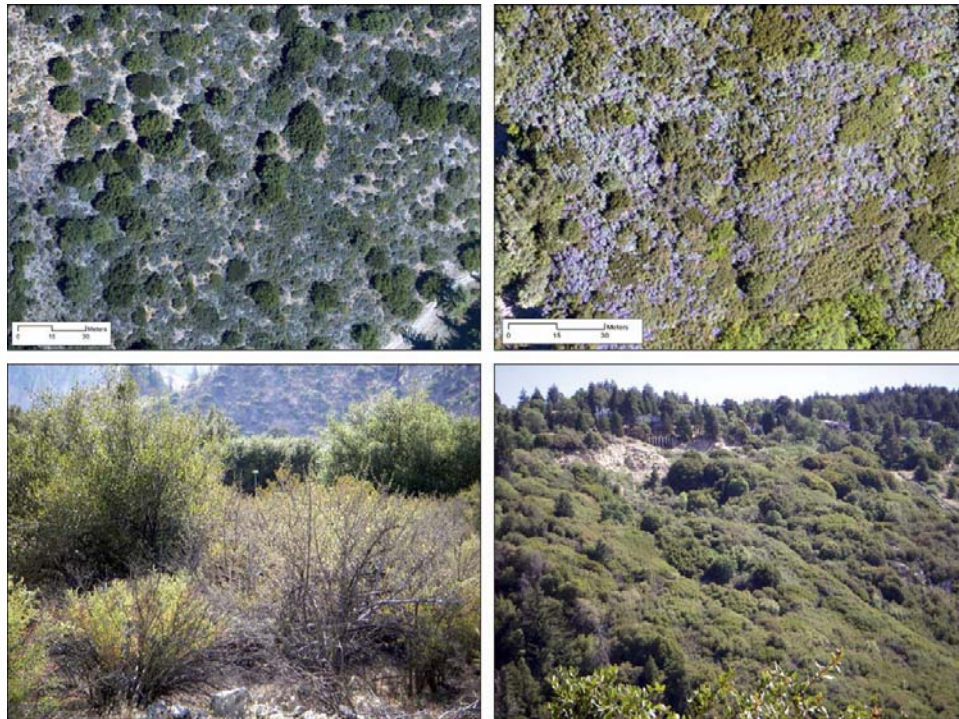


Figure 16. Overhead (top) and oblique views (bottom) of Grand Prix (left) and Old 2 (right) sites.



Figure 17. Overhead (left) and oblique (right) views of Piru site.



Figure 18. Field plot with GPS antenna located over a control point and measurement lines in place for plot measurements at the study site near the Grand Prix complex (GP1).

Methods

Data Fusion and Direct Comparison of LIDAR, IFSAR, and Field-Measured Vegetation Heights

LIDAR point data were processed using the FUSION software () to produce a bare-earth surface model. An independent accuracy assessment that compared the bare-earth surfaces and survey-grade dual frequency (L1/L2) real-time kinematic (RTK) GPS positions indicated that the overall error in the ground surface elevations averaged 4 cm (61 cm std. dev). In the highest density vegetation areas, LIDAR ground elevations were an average of 10 cm (69 cm std. dev.) above the RTK ground elevations. In areas with the tallest vegetation, LIDAR elevations were an average of 13 cm (70 cm std. dev.) above the RTK ground elevations (Cooke 2008). The LIDAR-derived bare-earth surface was used as the “true” ground surface thus allowing us to compute vegetation heights using both a LIDAR-derived canopy surface model and the IFSAR DEMs (see next section, LIDAR-derived Bare-earth Surface Assessment, for details on LIDAR ground surface accuracy) .

Visual assessment of the IFSAR DEMs revealed that the surface did not represent the bare-earth, as described by the LIDAR-derived bare ground surface model, or the top of the vegetation. Instead, the IFSAR DEM surface was located between these ground and the top of the vegetation. Figure 19 illustrates the relationship between the IFSAR DEM surface, a LIDAR-derived bare-earth surface and LIDAR point data.

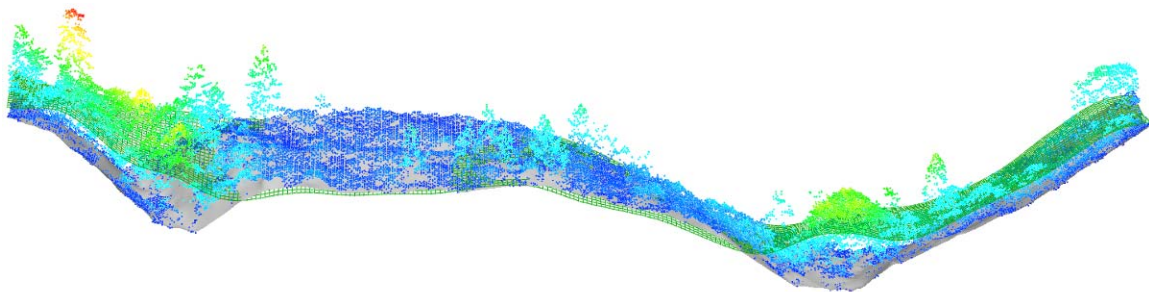


Figure 19. LIDAR bare-earth surface model (gray shaded surface), IFSAR DEM (green wireframe), and LIDAR laser returns colored by height above ground (blue is low veg height; red is high veg height).

LIDAR point data were also processed using FUSION to produce a canopy surface model. The algorithm assigns the highest laser return in the sample cell to the surface gridpoint representing the cell. Figure 20 shows the LIDAR bare-earth and canopy surfaces along with the LIDAR point cloud.

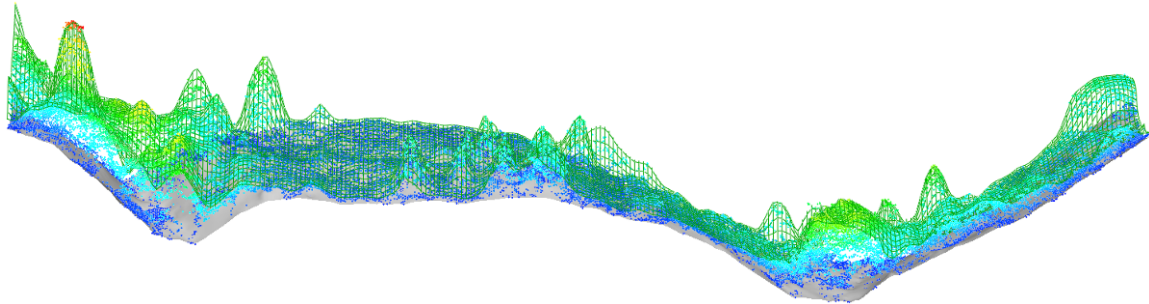


Figure 20. LIDAR bare-earth surface model (gray shaded surface), LIDAR canopy surface model (green wireframe), and LIDAR laser returns colored by height above ground.

Field measurements and plot corner locations were processed to produce a vegetation height measurement for each ground sample point within each plot. For plots measured using the grid method, the vegetation height measured at each sample point was used directly. For plots with mapped, individual tree data, the crown shape code was used in conjunction with the crown width measurements and location of the center of the tree crown to compute a vegetation height for all sample points within the footprint of the tree crown.

The complete data for each field plot included the location of the sample points for the plot and the corresponding field-measured vegetation heights, LIDAR-derived vegetation height, and IFSAR-derived vegetation height. These data were saved in comma separated value (CSV) format for use in statistical analyses. Figure 21 shows an example of the sample point data for two plots with all measurements represented as XYZ points. Vegetation heights for the plot shown on the left in Figure 21 were measured using a sample point grid and the plot contained stem-mapped trees. Heights for the plot shown on the right in Figure 21 were measured using only a sample point grid.

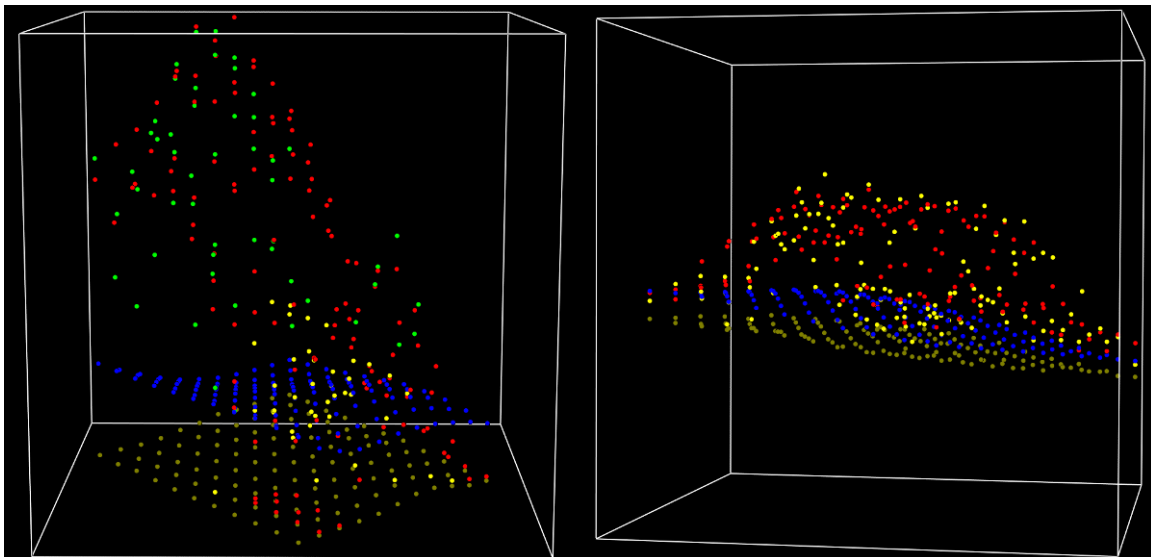


Figure 21. Point clouds representing the data for two sample plots. Point colors represent the source of the point data (Brown: LIDAR bare-earth, yellow: field-measured vegetation, green: stem-mapped tree, Red: LIDAR vegetation, Blue: IFSAR vegetation).

Table 3 presents a summary of the statistics computed for each plot. The tallest individual height measured on a plot was 34.60 m obtained from a stem mapped tree. For summary and analysis, the plots were grouped depending on the type of vegetation present on the plot and the method used to measure the vegetation heights.

Table 3. Summary of plot-level average vegetation heights. Statistics reported in the table are for plot-level averages.

Measurement protocol	Average plot-level vegetation height (m)	Standard deviation (m)	Min. (m)	Max. (m)
All plot types	3.82	4.11	0.00	13.36
Plots with stem-mapped trees	7.79	4.34	0.99	13.36
Plots with tree heights measured using grid	6.51	3.51	2.10	9.85
Plots with no trees	1.36	0.81	0.78	3.63
Plots with uniform vegetation height or no vegetation	0.88	0.88	0.00	2.50

LIDAR-derived Bare-earth Surface Assessment

Given the problems with processing and using the P-band IFSAR data, we acquired LIDAR data for a limited portion of the study area to test the usefulness of the X-band IFSAR data for measuring vegetation height. LIDAR-derived bare-ground surface have been found to be accurate in a variety of terrain and vegetation conditions (Reutebuch et al. 2003; Kraus and Pfeifer 1998). However, the low, dense vegetation common in these study areas presents special problems for laser measurement. For areas covered by dense vegetation one- to three-meters tall, it is not uncommon for the last returns from the laser pulse to fall on the surface of the vegetation or in the vegetation. Pulses either do not reach the ground (all energy is reflected from vegetation) or reflections from the ground are not detected by the receiver because the time required to process and store a return from the vegetation surface prevents the system detector from resetting before the energy reflected from the ground surface is received. This time delay translates into a one- to two-meter “blind spot” where the LIDAR receiver cannot detect a return. Streutker (2006) points out that the resolving ability of common LIDAR instruments is not discussed in the literature and Goodwin et al. (2006) mention that the Optech ALTM 3025 sensor cannot distinguish between first and last returns from objects within 4.9 meters of one another due to the circuitry used in the system. Advances in system design and processing capabilities have reduced, but not eliminated, this “blind spot”.

To assess the accuracy of bare-ground models in chaparral, we funded a graduate student at the University of Washington (UW) (Andrew Cooke) to conduct a study to assess whether or not LIDAR laser pulses penetrate the vegetation and provide an accurate measurement of the ground surface and to determine whether or not the

height and density of vegetation have an effect on the accuracy of LIDAR-derived ground models (Cooke 2008). A survey-grade dual frequency (L1/L2) real-time kinematic GPS survey of five research sites in the San Bernardino and Los Padres National Forests with vegetation cover ranging from low shrubs with grass to dense, mature chaparral was undertaken in June 2007. Measurements of ground elevation, vegetation height, and vegetation density were taken at 1,709 points, and these measurements were compared to LIDAR data collected in August of 2005. Methods were used to adjust for vegetation growth from 2005 to 2007 and systematic differences between the LIDAR and GPS data (Cooke 2008).

Vegetation height was measured to the nearest five centimeters by reading where the tallest vegetation contacted the side of the height pole. If vegetation was over three meters, a position was taken with the height recorded as greater than three meters. Vegetation density was measured by observing the one meter diameter circle centered on the height pole, and estimating how much vegetation was within the circle. The classes, shown in Table 4, were established to describe the density. These classes were intentionally broad given the difficulty of having multiple observers provide the same estimate.

Table 4. Vegetation density classes used to characterize the amount and density of the vegetation at each GPS point.

Density class	Amount of Observed Vegetation
0	None or nearly none
1	Some
2	A lot

To characterize the height growth between the field measurements collected in 2007 and the LIDAR acquisition in 2005, 75 RTK points were measured within three of the plots measured in 2005. A 2- by 2-meter grid of points in these three plots were surveyed in 2005 to obtain a ground elevation and vegetation height. This survey was completed in addition to the measurements described in Field Data section above. The vegetation heights measured in 2005 were used to create a surface which was then used to interpolate a 2005 vegetation height using the horizontal location of the 2007 RTK points. The difference between the two vegetation heights was assumed to be the result of growth. This growth estimate was subtracted from the 2007 heights to obtain an estimate of vegetation height at each point in 2005. For the 75 GPS points taken within the three 2005 field plots, it was determined, using this method that the average vegetation growth between when the LIDAR was flown in 2005 and when the GPS data were collected in 2007, was 0.54 meters \pm 0.53 meters. 0.54 was subtracted from the 2007 vegetation heights to estimate 2005 vegetation heights.

One of the most common products derived from LIDAR data is a bare-ground surface model. Processing methods used to identify returns from the ground surface generally assume that the LIDAR point cloud contains a substantial number of points that represent reflections from the ground surface. In the dense vegetation characteristic of our study sites, this assumption may not be valid. In many cases, there are very few returns that represent the ground. There are often so many returns at the top of the 1- to

3-meter tall vegetation that the actual ground returns appear to be outliers. The LIDAR acquisition for this study included identification of the bare-earth returns within the point cloud. However, the conditions made this task especially difficult. The data provider identified ground points using a proprietary algorithm implemented in the TerraScan commercial LIDAR processing software. Detailed evaluation of the filtering results led us to conclude that the bare-ground surfaces might not represent the “true” ground surface. As part of the UW thesis work, a new algorithm was developed that provided the most likely ground surface for the area at the horizontal location of the RTK GPS points. This algorithm did not attempt to create a complete wall-to-wall surface but rather focused on identifying the best ground elevation for each of the 1,709 RTK-GPS sample locations.

IFSAR P-band Bare-earth Surface Assessment

The restrictions imposed by the FCC on the frequencies used by P-band IFSAR prevent processing of the backscatter information to produce P-band bare-ground surface models for the SoCAL project areas. However, an earlier acquisition in Western Washington collected without these restrictions allowed evaluation of the accuracy of P-band ground surfaces.

The study area for this project was a 5.2 km² area within Capitol State Forest in western Washington State, USA. The forest was primarily composed of coniferous Douglas-fir (*Pseudotsuga menziesii*), western hemlock (*Tsuga heterophylla*), and, to a lesser degree, hardwoods such as red alder (*Alnus rubra*) and maple (*Acer* spp.). The site is located in a mountainous area, with elevations ranging from 150 to 400 m and ground slopes varying from 0% to 83%. As part of an experimental silvicultural trial, this 70 year old forest was partially harvested in 1998, resulting in units falling into four different residual canopy density classes (Curtis et al., 2004). The residual stand density is 0 trees per hectare (TPH) in clearcut units; in heavily thinned units, approximately 40 TPH remain, dominant height is 43.5 m, and quadratic mean diameter (QMD) is 59.2 cm; in lightly thinned units, approximately 175 TPH remain, dominant height is 44.4 m, and QMD is 56.6 cm; and in the uncut units, 280 TPH remain, dominant height is 47.3 m, and QMD is 52.6 cm.

Three hundred and forty-seven (347) topographic checkpoints located in the central part of the study area were surveyed using a Topcon ITS-1 total station surveying instrument. A large proportion (85%) of the checkpoints was under forest canopy. The ground survey was made up of three closed traverses that started at reference points established using a survey-grade global positioning system (GPS). Upon adjustment of the traverses, the accuracy of the checkpoints was approximately 3 cm vertical and 15 cm horizontal.

IFSAR data were collected over the study areas in September 2002 using the TopoSAR X- and P-band system (formerly AeS- 1, developed by Aerosensing Radarsysteme GmbH, and now owned and further developed by Intermap Technologies Corp.). In the case of P-band, the 2.5 m data were acquired within overlapping swaths from four orthogonal viewing directions. The vendor provided a digital terrain model (DTM)

generated from an optimized integration of the fully polarimetric P-band data. Using the fact that polarimetric response varies between different components of the canopy-ground system, an internally developed coherence optimization scheme was developed by researchers at Intermap Technologies Corp. (Mercer, 2004). This methodology assumed that the polarization state corresponding to the optimum coherence in forested areas is associated with the ground response. It should be noted that, although the DTM post spacing was 2.5 m, application of a smoothing function reduced the effective independent spacing width by several meters.

IFSAR X-band Vegetation Height Assessment

A study to assess the accuracy of canopy heights derived from X-band IFSAR and the effect of flight parameters, interferometric processing, slope and canopy density was conducted using data collected over a 5 km² area within Wenatchee National Forest. The study site is located in the Mission Creek drainage within the eastern Cascade mountains of Washington State (part of the JFSP FFS Mission Creek area). This is a mixed-conifer forest, composed primarily of mature Douglas-fir, ponderosa pine, grand fir (*Abies grandis*), and various shrub species. This area is mountainous, with slopes in forested areas ranging from 0–50°. Since the focus of this study was on the accuracy of IFSAR canopy measurements, and not terrain measurements, a GIS polygon layer of vegetation cover type was used to isolate and restrict the analysis to the forested regions within the study area.

For this study, LIDAR data were acquired to provide a bare-ground surface that could be used to derive vegetation heights from the IFSAR X-band canopy surface. In addition, the LIDAR data were processed to produce a canopy surface model that could be compared directly to the IFSAR-derived canopy surface. The LIDAR data used in this study were acquired in the summer of 2004 with an Optech ALTM 3070 system mounted on a fixed-wing aircraft. This system acquired data with a pulse rate of 70 kHz, and provided data at a nominal density of 4 points/m².

Ground returns were filtered by the vendor and were used to interpolate a 1m by 1m resolution gridded digital terrain model (Fig. 22). Lidar returns from the canopy surface were identified by filtering out the highest return within a 1m by 1m grid cell. A 1.25m by 1.25m resolution canopy surface model was then interpolated using these filtered, canopy-level returns (Fig. 23).



Figure 22. Lidar-derived terrain surface model for a portion of the Mission Creek study area, Wenatchee National Forest, Washington State, USA. Area is approximately 500m by500 m, and the view is looking west to east.

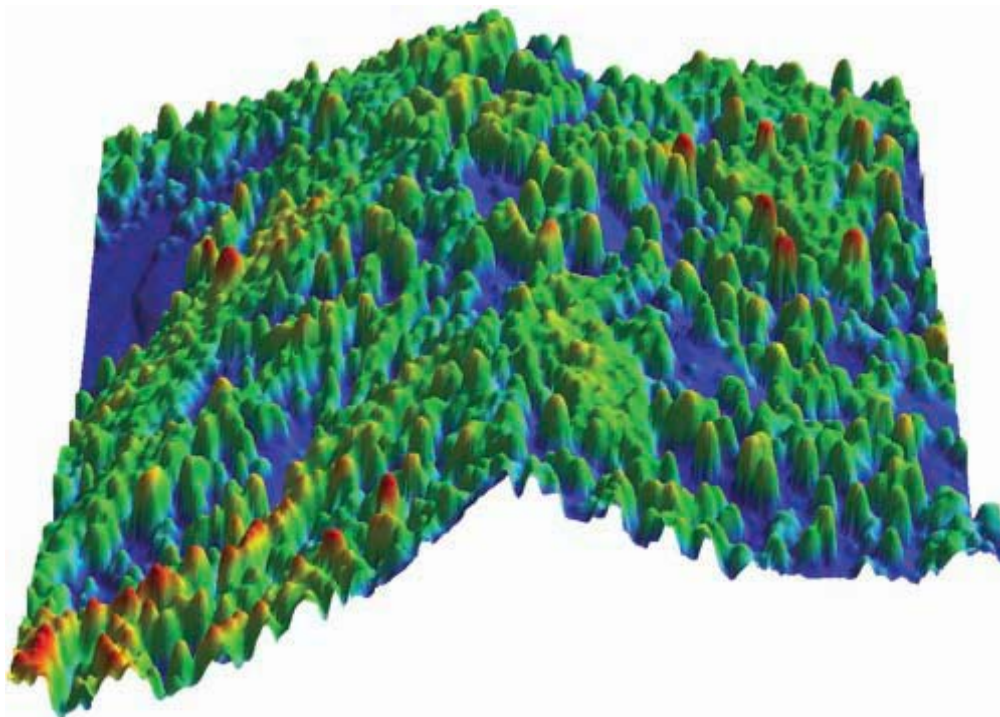


Figure 23. Lidar-derived forest canopy surface model (same area as Figure 22). Color-coded by height (blue is low canopy, red is high canopy).

IFSAR data were acquired in the summer of 2005 with the Intermap Star 3i X-band system, operating from a Lear jet aircraft platform. The wavelength for this system was 3.1 cm, and the flying speed was 720km/h.

In order to assess the effect of flying height on the accuracy of IFSAR canopy measurements, data were collected from both 15,000 ft (approx. 4500 m) and 20,000 ft (approx. 6000 m). Additionally, the IFSAR data were processed by the vendor using four different levels of interferogram filtering, or levels of oversampling (OSF). The highest level of filtering (OSF factor of 8) represents the standard (default) processing parameter for the 5-m digital surface models, and has a filtering window of slightly greater than 5 m. An OSF factor of 1 corresponds to no filtering, so the fundamental pixel size is 1.25 m, and OSF factors of 2, 4 and 8 correspond to increasing levels of filtering. Three flight lines, from one look direction, were acquired from 6000 m, and 13 flight lines, from three orthogonal look directions, were acquired from 4500 m. Three-dimensional perspective view of the IFSAR canopy surface model (combination of all looks, OSF 8, 4500m flying height) for a selected area within the study site is shown in Figure 24.

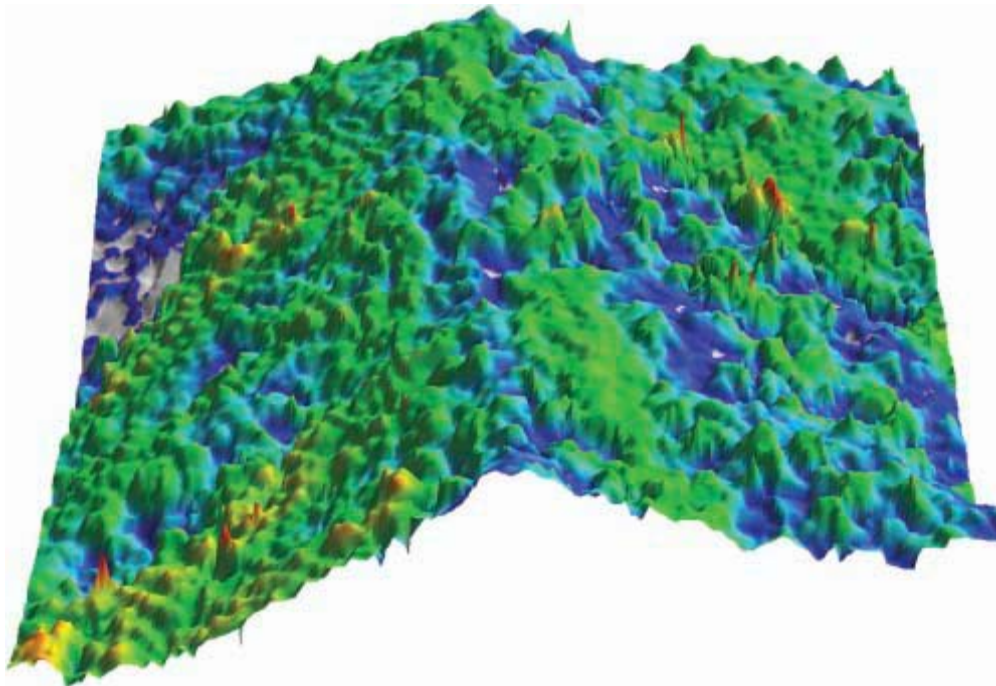


Figure 24. IFSAR-derived forest canopy surface model (same area as Figure 22). Color-coded by height (blue is low canopy, red is high canopy)

Results and Discussion

Direct Comparison of LIDAR, IFSAR, and Field-Measured Vegetation Heights

Tables 5 and 6 summarize differences between the average vegetation height for plots measured in the field and the average height for the same area derived from LIDAR and IFSAR canopy surfaces.

Table 5. Difference between average vegetation height for plots and average LIDAR-derived vegetation height for plots (Field height – LIDAR height).

Measurement protocol	Mean height difference (m)	Standard deviation (m)	Min. (m)	Max. (m)
All plot types	-1.25	2.27	-9.07	0.70
Plots with stem-mapped trees	-3.71	2.70	-9.07	-0.25
Plots with tree heights measured using grid	-1.35	0.80	-2.49	-0.63
Plots with no trees	-0.07	0.44	-1.04	0.40
Plots with uniform low vegetation height or bare ground	0.24	0.46	-0.39	0.70

Table 6. Difference between average vegetation height for plots and average IFSAR-derived vegetation height for plots (Field height – IFSAR height).

Measurement protocol	Mean height difference (m)	Standard deviation (m)	Min. (m)	Max. (m)
All plot types	1.56	2.13	-6.62	5.97
Plots with stem-mapped trees	1.99	3.46	-6.62	5.97
Plots with tree heights measured using grid	0.19	1.69	-1.20	2.23
Plots with no trees	1.76	0.59	0.93	2.64
Plots with uniform low vegetation height or bare ground	1.41	1.46	-1.53	2.78

In general, LIDAR-derived heights are greater than the heights measured in the field and IFSAR-derived heights are lower than those measured in the field. Figure 25 shows a box plot for the average plot heights. Close examination of the data indicates that most of the large LIDAR height differences occur in areas with stem-mapped trees. The procedure for mapping trees in the field involved locating the center of the tree crown and then measuring two crown widths from this center location. A shape code was assigned to each tree to characterize the overall crown shape. These measurements were then used to model the tree crown and populate grid points with an associated vegetation height. While this procedure was reasonable efficient in the field, it did not

always produce perfect results. Trees seldom have perfectly shaped crowns. LIDAR typically measures all surfaces with area sufficient to reflect the laser energy. The crown volumes represented in the LIDAR point cloud were often irregular and significantly different from the simple geometric shape assigned to a tree. The net effect of this difference was that the LIDAR and field measurements were often significantly different. In contrast the LIDAR, RADAR tends to “smooth” the canopy surface resulting in a canopy surface model that falls somewhere between the ground and the top of the actual canopy. Comparisons between the IFSAR and LIDAR surfaces and the field measurements reveal that the IFSAR seldom measures the top of the vegetation. In addition, the IFSAR surface tends to be very smooth when compared to a LIDAR surface. This smoothing effect is particularly evident when the vegetation height changes significantly over a short horizontal distance. The height change can be the result of vegetation differences, e.g. large gap in a the tree cover, or due to topographic features. Figure 26 shows the data for a plot located on a topographic bench with no vegetation cover (gravel road turnout). The bench was situated on a roughly 45-degree slope with tall trees on two sides of the plot. The IFSAR canopy surface (green mesh in Figure 26 C and D) shows the influence of the surrounding trees and topography. In particular, the tree circled in yellow in Figure 26 A and D “lifted” the surface above the bare ground near the upper edge of the plot.

When we compared the individual point measurements, LIDAR vegetation height was an average of 1.17 m taller than the field measurement and IFSAR height was an average of 1.56 m lower than the field height. Figure 27 shows a box plot for the individual height measurements.

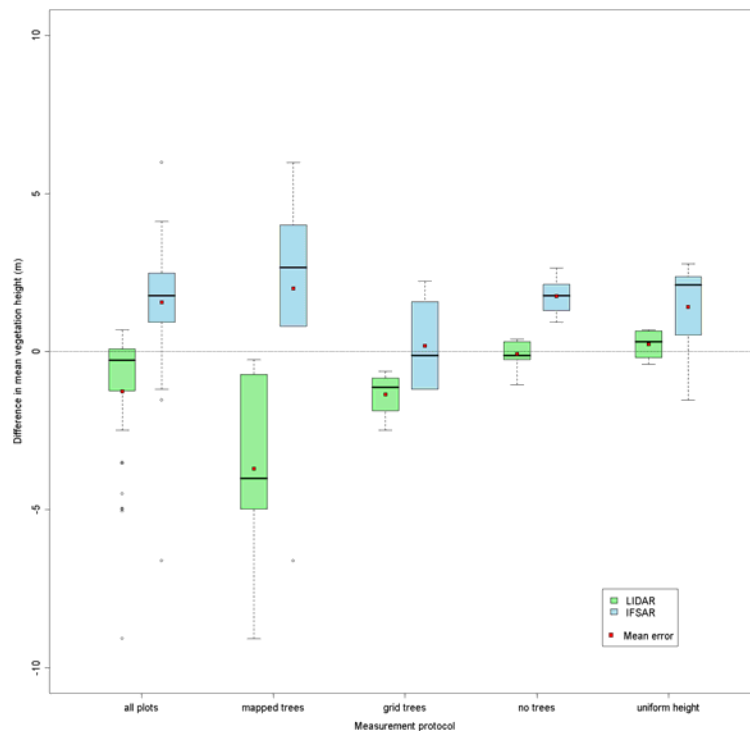
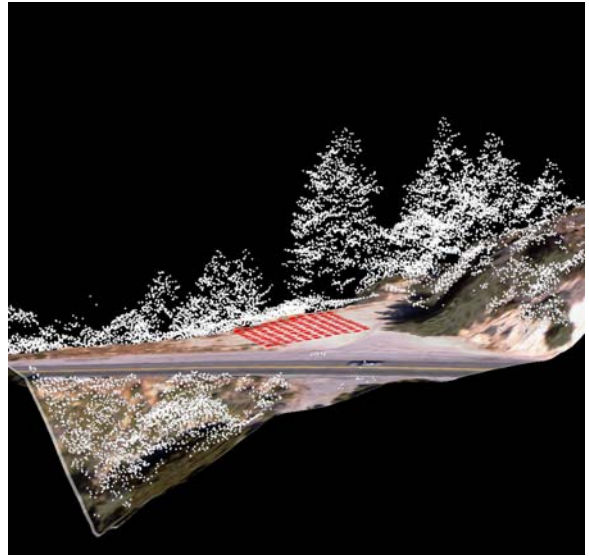


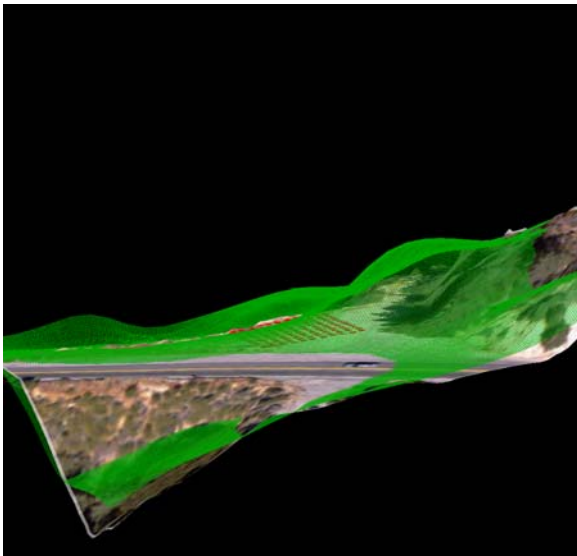
Figure 25. Box plot showing the average plot error in vegetation height.



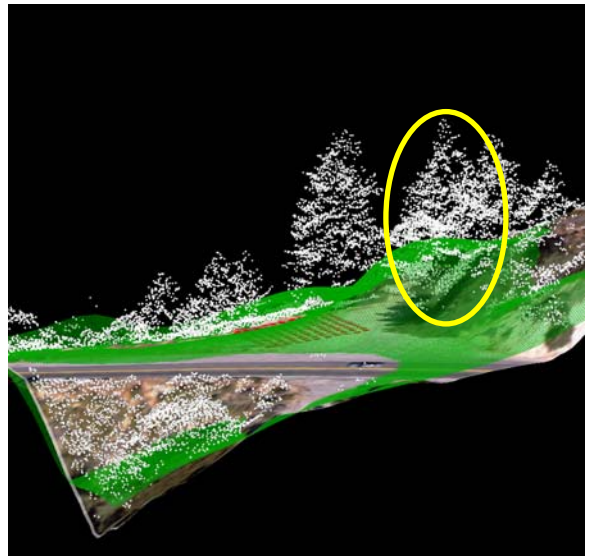
A



B



C



D

Figure 26. Field plot showing the effect of vegetation on the IFSAR canopy surface. Image A shows the location of the field measurement points. Image B shows an oblique of the LIDAR-derived ground surface model with the LIDAR data points in white. Image C shows the IFSAR canopy surface in green. Image D shows the IFSAR canopy surface (green) and the LIDAR points (white).

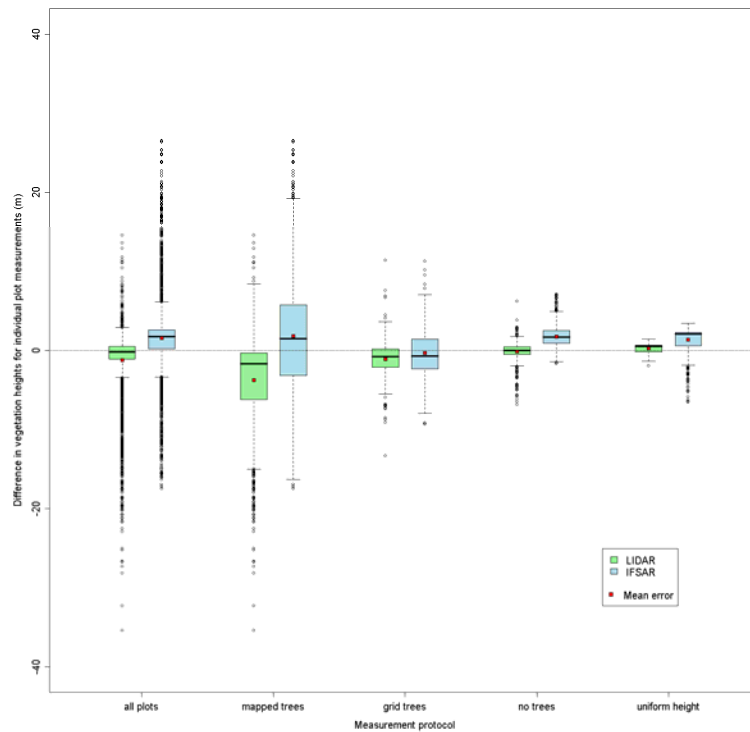


Figure 27. Box plot showing the error in vegetation height for individual measurement points.

LIDAR-derived Bare-earth Surface Accuracy

Table 7 summarizes the 1,709 field points that were collected to assess the accuracy of the LIDAR-derived bare-ground surface. The “Veg RTK” points were points collected while using RTK-GPS mode and the “Veg non-RTK” were points collected without RTK enabled. For the non-RTK points, 60 epochs were collected for each location and the results post processed to produce accurate locations. Overall the LIDAR ground elevations were 0.04 ± 0.61 meters above the GPS ground elevations. In the highest density vegetation, the LIDAR ground elevations were 0.10 ± 0.69 meters above the GPS ground elevations, and this increased to 0.13 ± 0.70 meters in the tallest vegetation category.

Table 7. Number of GPS points by vegetation height and vegetation density at each study site.

Site	Point Type	Categorized 2007 Height				Density		
		0-1m	1-2m	2-3m	>3m	0	1	2
Old1	Veg RTK	82	195	62	15	27	164	163
	Veg non-RTK	8	9	1	0	2	12	4
Old2	Veg RTK	2	28	75	22	0	51	76
	Veg non-RTK	1	26	5	0	0	0	32
Grand Prix	Veg RTK	42	125	74	22	10	72	181
	Veg non-RTK	0	0	0	0	0	0	0
Piru2	Veg RTK	59	159	131	17	14	202	150
	Veg non-RTK	14	59	5	6	0	31	53
Piru1	Veg RTK	103	271	57	15	30	300	116
	Veg non-RTK	1	18	0	0	0	10	9

Table 8 summarizes the results for RTK vegetation GPS points, non-RTK vegetation GPS points, and the GPS points categorized by their field-recorded density. It also summarizes results for points broken down into one meter vegetation height categories. The “greater than three meter height” category could not be adjusted by subtracting the vegetation growth, because true heights at those points could not be measured in the field. Therefore, the results are the same in this height category for both 2007 and 2005 heights.

Table 8. Ground elevation differences (LIDAR-GPS) for vegetation GPS points, in meters.

		Category	Mean	Std. Dev.	# of Points
		All Points	0.043	0.613	1709
		RTK Points	0.042	0.601	1556
		Non-RTK Points	0.058	0.726	153
		Density 0 Points	-0.060	0.374	83
		Density 1 Points	-0.003	0.549	842
		Density 2 Points	0.104	0.688	784
Vegetation Height	2007	Height 0-1m Points	-0.032	0.477	312
		Height 1-2m Points	0.030	0.581	890
		Height 2-3m Points	0.133	0.699	410
		Height >3m Points	0.031	0.822	97
	2005	Height 0-1m Points	-0.002	0.493	862
		Height 1-2m Points	0.091	0.688	586
		Height 2-3m Points	0.118	0.725	164
		Height >3m Points	n/a	n/a	97

In addition to the field campaign, a simulation study was conducted to examine the underlying error in GPS positions given the accuracy of the GPS receivers used to collect positions and the post-processing procedures followed. Overall, the errors summarized in Table 8 exceed those that would be attributable to GPS accuracy alone indicating that the presence of dense, short or medium height vegetation influences the accuracy of the LIDAR-derived bare-ground surface. The overall trend is that as

vegetation height and density increase, the ability of the laser pulse to reach the ground is compromised. Based on the LIDAR-GPS height differences observed in this study, vegetation heights could be underestimated by 0% to 9%. However, the overall accuracy of the LIDAR-derived ground surface is still very high and is better than any other remotely sensed ground elevation measurement technique.

IFSAR P-band Bare-earth Surface Accuracy

For the western Washington study area, the elevation of the DTM at the position of each ground-surveyed elevation checkpoint was calculated using bilinear interpolation. The difference between the two elevations (DTM minus checkpoint) was then calculated as the DTM error. Figure 28 shows the distribution of the DTM errors. The mean of the elevation differences between the IFSAR DTM and the 347 checkpoints was -0.28 ± 2.59 m (mean \pm SD). The RMSE was calculated as 2.60 m. For the purposes of comparison, the accuracy of the standard USGS 10 m DTM was also evaluated using the same topographic checkpoints. The mean error of the USGS DTM was found to be 7.3 ± 4.9 m (mean \pm SD), with a maximum observed error of 18.07 m and a minimum of -4.91 m. The RMSE of the USGS DTM was calculated as 8.8 m. Interestingly, this was quite close to the accuracy of approximately 9 m reported in Carson and Reutebuch (1997).

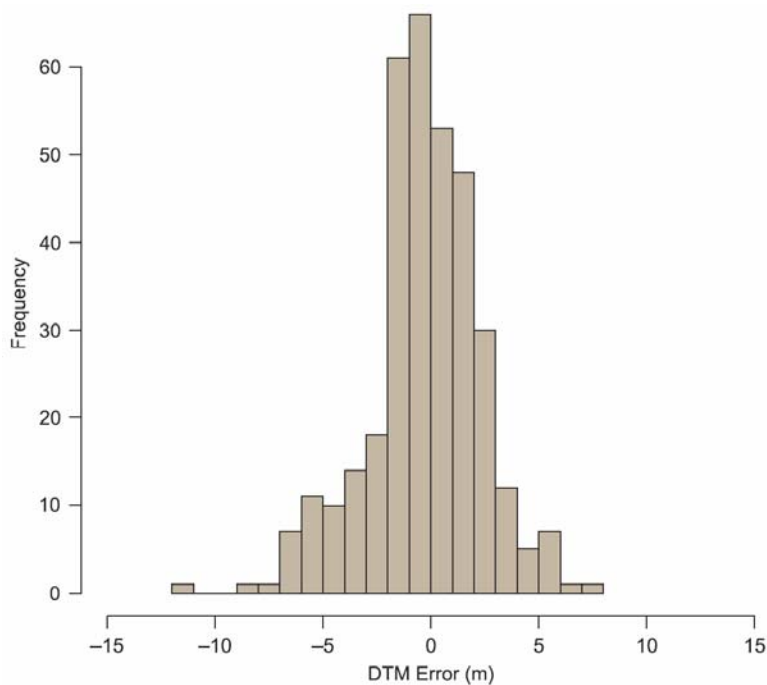


Figure 28. Distribution of IFSAR P-band DTM error compared with 347 surveyed checkpoints.

The checkpoints were assigned to four canopy classes, and checkpoints falling on unit boundaries were eliminated, leaving 326 points. Summary statistics of the DTM error in each canopy class are given in Table 9. While the mean error was negative for all treated units (i.e., DTM under the true terrain elevation), in the uncut unit the mean error was positive. The standard deviation of the error also tended to increase with increased

canopy density (although there is little difference between clearcut and heavily thinned). The range of errors also tended to increase with higher canopy densities.

Table 9. IFSAR DTM elevations minus surveyed checkpoint elevations, segregated by canopy density class.

Canopy class	Mean (m)	SD (m)	RMSE (m)	Min. (m)	Max. (m)	No. of checkpoints
Clearcut	-0.67	1.20	1.38	-3.34	2.34	38
Heavily thinned	-0.62	1.00	1.18	-2.48	1.49	21
Lightly thinned	-0.41	2.32	2.36	-7.05	6.00	147
Uncut	0.20	3.31	3.32	-11.13	7.36	120

Summary statistics for DTM error classified by slope class are shown in Table 10. Although mean error for low slopes (<19%) was negative (-0.60 m) and the mean error for high slopes (>19%) was positive (+0.21 m), the difference between the standard deviations of the error was negligible (2.57 m versus 2.58 m). The RMSE difference between the slope classes was also minimal (2.64 m versus 2.59 m).

Table 10. IFSAR DTM elevations minus surveyed checkpoint elevations, segregated by slope class.

Slope class	Mean (m)	SD (m)	RMSE (m)	Min. (m)	Max. (m)	No. of checkpoints
Low slopes (<19%)	-0.60	2.57	2.64	-11.13	5.51	177
High slopes (>19%)	0.21	2.58	2.59	-7.05	7.36	149

IFSAR X-band Vegetation Height Accuracy

Influence of Flying Height during IFSAR Data Acquisition

The summary statistics of the IFSAR error (IFSAR height – LIDAR height) associated with single passes at 6,000m and 4,500m flying heights are shown in Table 11. The study area was located close to the center of the swath for both flight lines, and only the elevations obtained via the standard interferometric processing settings (OSF of 8) were used in the comparison. Quartile deviation (QD) was computed as one half of the difference between the 75th percentile height and the 25th percentile height. Quartile deviation is a measure of variability that is less influenced by extreme observations than standard deviation.

Table 11. Differences between IFSAR- and lidar-derived height estimates for 4,500m and 6,000m flying heights for IFSAR data collection, using data from single passes at each height and an oversampling factor of 8 (IFSAR-lidar).

Flying Height AGL* (m)	Canopy height (m)				Maximum height (m)			
	Mean	SD	Median	QD	Mean	SD	Median	Qd
6,000m	-7.5	4.9	-7.2	2.9	-10.7	6.9	-10.3	2.9
4,500m AGL	-7.0	4.9	-6.7	2.8	-10.2	6.3	-9.9	3.6

* AGL, above ground level.

Influence of Filtering Parameters

The summary statistics for IFSAR elevations generated using the four different levels of interferogram filtering for a single flight line are shown in Table 12. Only the elevations obtained from the lower flying height (4,500m) were used in this comparison.

Table 12. Differences between IFSAR- and LIDAR-derived height estimates using data from a single pass acquired at a 4500m flying height with four different levels of interferogram filtering (IFSAR-LIDAR).

	Canopy height (m)				Maximum height (m)			
	Mean	SD	Median	QD	Mean	SD	Median	Qd
OSF* 1	-6.5	4.4	-6.1	2.2	-1.6	9.6	-2.5	4.4
OSF 2	-6.5	4.5	-6.0	2.3	-2.7	9.5	-3.3	4.3
OSF 4	-6.5	4.6	-6.1	2.5	-4.1	8.6	-4.6	4.3
OSF 8	-7.0	4.9	-6.7	2.8	-10.2	6.3	-9.9	3.6

* OSF, oversampling factor.

Influence of Sensing Geometry

A previous study has indicated that using a combination of IFSAR elevations obtained from different look directions can improve canopy height models (Andersen et al. 2003). In order to reduce the underestimation of canopy height due to shadowing effects, the IFSAR elevations obtained from overlapping flight lines were merged by extracting the maximum elevation within each grid cell. The error associated with the merged surfaces obtained from overlapping flight lines with the same look directions, opposite look directions, orthogonal look directions, and all look directions are compared in Table 13.

Table 13. Differences between IFSAR- and LIDAR-derived height estimates. IFSAR collected at multiple passes at 4,500m flying height (two side looks from same direction, two orthogonal looks, opposite look directions, and combination of all looks). Oversampling factor of 8 (IFSAR-LIDAR).

	Canopy height (m)				Maximum height (m)			
	Mean	SD	Median	QD	Mean	SD	Median	Qd
Side looks	-3.2	4.9	-3.2	2.9	-5.4	7.5	-5.8	3.6
Opposite looks	-2.2	3.5	-2.5	2.0	-4.4	5.5	-5.0	2.6
Orthogonal looks	-1.6	4.1	-1.6	2.1	-3.4	7.1	-4.2	2.8
All looks	-0.6	3.9	-0.8	2.0	-2.1	7.1	-3.2	2.9

Influence of Slope

Due to the relatively shallow look angles characteristic of radar imaging, the accuracy of IFSAR canopy measurements could be influenced by terrain slope. A previous study has indicated that the influence of slope on the underestimation of canopy heights in X-band IFSAR is more pronounced in low-density stands (Izzawati et al. 2006). In addition, it was found that the influence of slope on X-band canopy height measurements is highly sensitive to the relationship between the radar viewing angle and the local slope characteristics (Izzawati et al. 2006). For example, when the radar system is viewing a slope at a very high off-nadir angle, lower parts of the tree crowns are making an increasing contribution to canopy height measurements, leading to underestimation of canopy height. Therefore, it can be expected that the influence of slope on the accuracy of X-band IFSAR canopy measurements will be largely mitigated by the use of canopy models developed from multiple passes with different look directions. Table 14 shows the influence of slope on canopy height measurements for a single pass, while Table 15 shows the influence of slope on canopy height measurements for surfaces obtained from all look directions.

Table 14. Differences between IFSAR- and LIDAR-derived height estimates across a range of slope classes. IFSAR collected on a single pass at 4500m flying height with an oversampling factor of 8 (IFSAR-LIDAR).

Slope class	Canopy height (m)				Maximum height (m)			
	Mean	SD	Median	QD	Mean	SD	Median	Qd
0–10°	-5.7	2.7	-5.9	1.6	-7.8	5.1	-8.4	2.9
10–20°	-5.7	3.4	-5.5	1.9	-8.3	4.4	-8.6	2.5
20–30°	-6.6	4.3	-6.3	2.6	-9.4	5.4	-9.0	3.3
30–40°	-7.3	5.3	-7.2	3.0	-10.8	6.9	-10.6	4.0
40–50°	-8.5	5.6	-7.4	3.8	-11.7	6.6	-11.1	3.6

Table 15. Differences between IFSAR- and lidar-derived height estimates across a range of slope classes. IFSAR generated from a combination of all looks acquired at a flying height of 4500 m with an oversampling factor of 8 (IFSAR-LIDAR).

Slope class	Canopy height (m)				Maximum height (m)			
	Mean	SD	Median	QD	Mean	SD	Median	Qd
0–10°	-2.9	1.8	-3.2	0.8	-3.1	6.5	-4.5	3.5
10–20°	-2.1	2.9	-2.3	1.5	-4.0	5.3	-5.2	2.4
20–30°	-0.9	3.3	-1.1	1.8	-2.5	7.3	-3.6	2.5
30–40°	-0.2	4.1	-0.3	2.1	-1.7	7.7	-2.7	3.0
40–50°	-0.2	4.3	0.5	2.6	-0.7	5.6	-1.1	3.3

Influence of Canopy Density

Previous studies have indicated that canopy density is a dominant factor influencing the accuracy of X-band IFSAR forest height measurements, where the degree of underestimation is inversely related to canopy density (Izzawati et al. 2006). In order to assess the influence of canopy density on the accuracy of IFSAR canopy heights, differences between IFSAR- and lidar-derived height models were grouped by canopy density class (derived from lidar) and summarized in Table 16.

Table 16. Differences between IFSAR- and lidar-derived height estimates across a range of lidar-derived canopy density (% canopy cover, or %CC) classes. IFSAR generated from a combination of all looks acquired at a flying height of 4500 m, with an oversampling factor of 8 (IFSAR-LIDAR).

%CC	Canopy height (m)				Maximum height (m)			
	Mean	SD	Median	QD	Mean	SD	Median	Qd
0–10	5.7	4.1	4.9	2.8	3.1	12.8	1.1	6.2
10–20	2.7	4.5	2.0	2.7	-2.9	6.5	-4.0	3.0
20–30	0.8	7.7	0.6	2.8	-1.6	8.3	-1.8	4.2
30–40	-0.0	5.4	-0.1	3.2	-1.2	9.0	-2.9	4.2
40–50	0.3	5.8	0.2	2.8	1.0	13.2	-0.8	4.2
50–60	-1.0	5.2	-1.4	2.7	-1.1	8.0	-2.5	3.7
60–70	-0.7	3.4	-1.0	2.1	-0.8	9.2	-2.7	3.2
70–80	-1.1	3.3	-1.3	2.2	-1.9	6.4	-3.1	2.8
80–90	-0.8	3.1	-0.8	1.7	-3.0	5.4	-3.7	2.5
90–100	20.5	2.6	20.6	1.5	22.7	3.6	23.1	2.2

Graphical Comparison of Canopy Height Models

A 370-m long transect (Figure 29) was selected for use in a graphical comparison of the IFSAR- and lidar-derived canopy height information. Figure 30 shows a comparison of a high-resolution, all-look IFSAR-derived canopy model (with the 5-m threshold for canopy cover estimation also shown). Figure 31 shows a comparison of the corresponding generalized canopy height (i.e. 90th percentile height) models at a 30-m resolution, and Figure 29 shows a comparison of the corresponding maximum height models at a 30-m resolution.

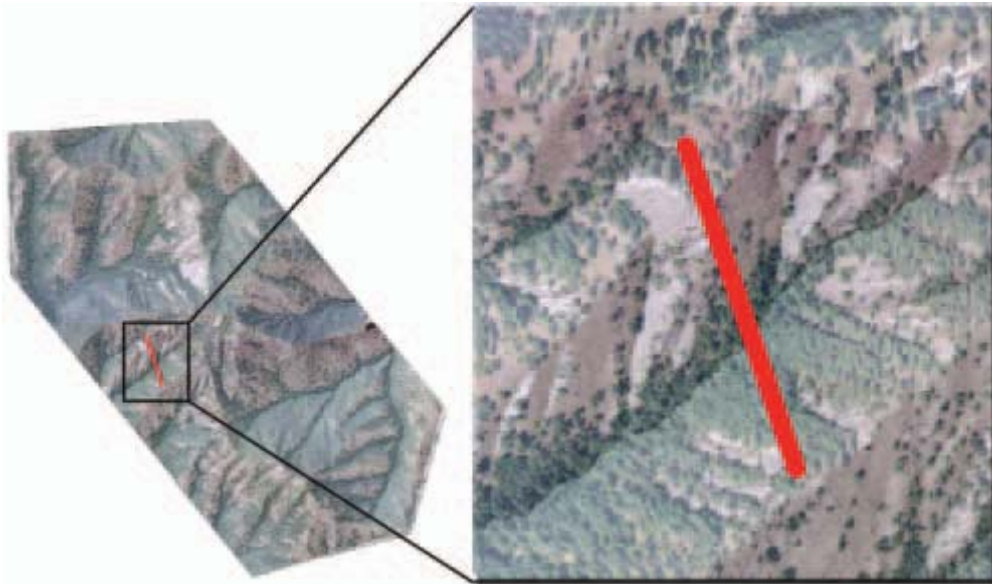


Figure 29. Location of 370-m-long transect within Mission Creek study area, Wenatchee National Forest, Washington State, USA.

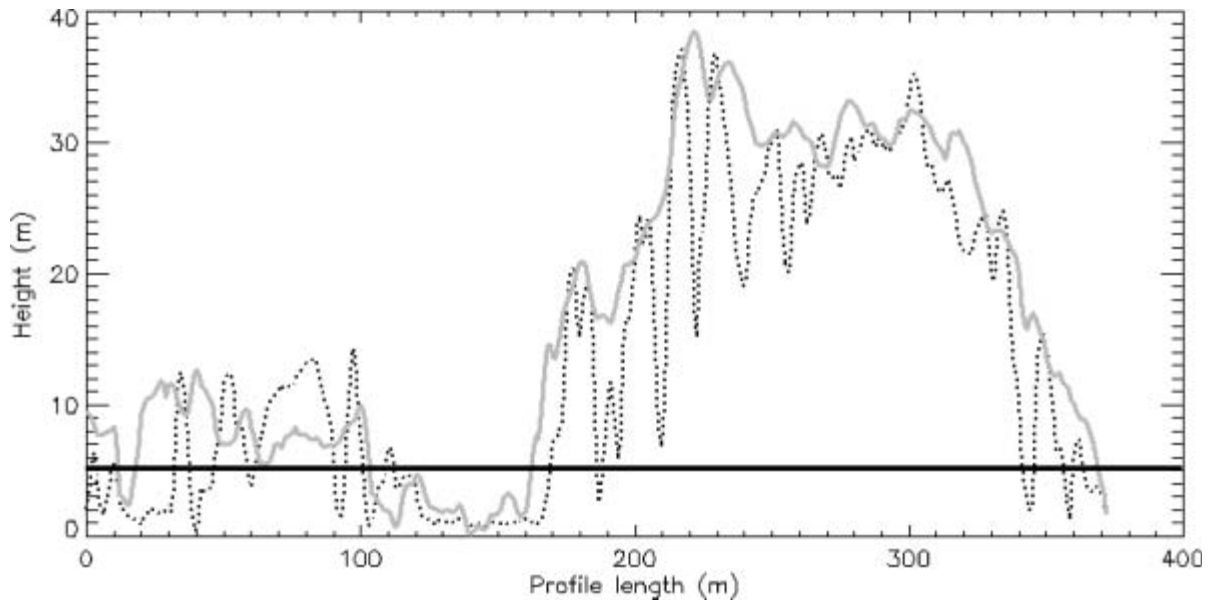


Figure 30. Comparison of high-resolution (1.25 m) canopy height models obtained from all-look IFSAR data (4500m flying height, oversampling factor of 8) and LIDAR along length of transect. IFSAR surface shown as solid gray line; LIDAR surface is shown as dotted line. 5-m threshold height for calculation of canopy cover is also shown as a bold black line.

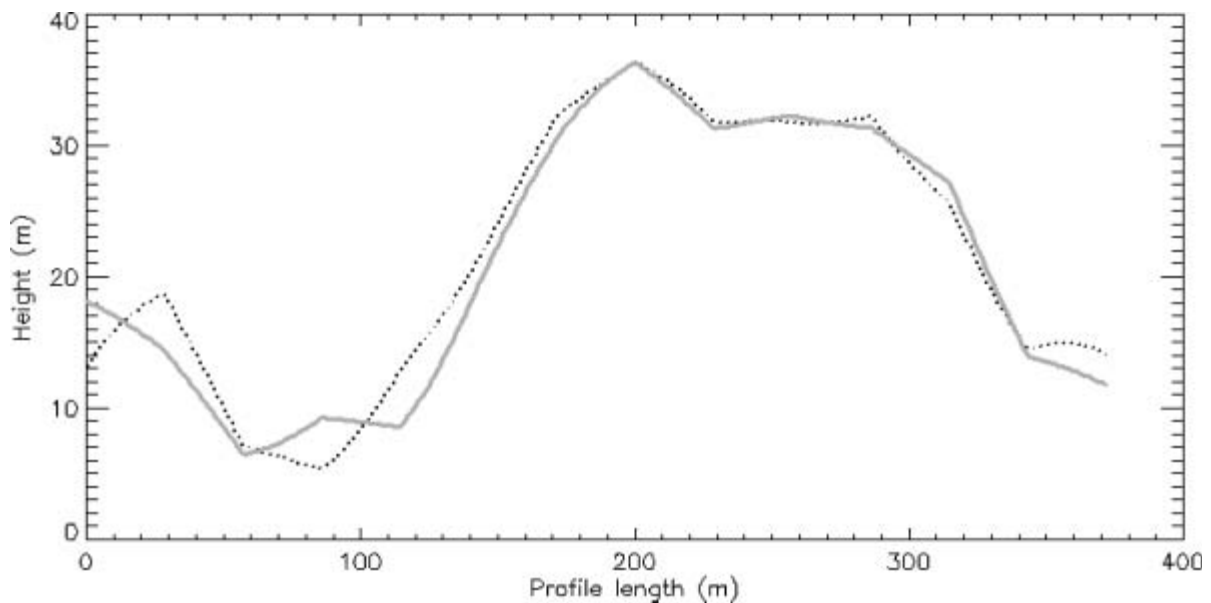


Figure 31. Comparison of generalized canopy height (90th percentile height within 30m grid cell) for IFSAR and LIDAR over length of transect. IFSAR surface shown as solid grey line; LIDAR surface is shown as dotted line.

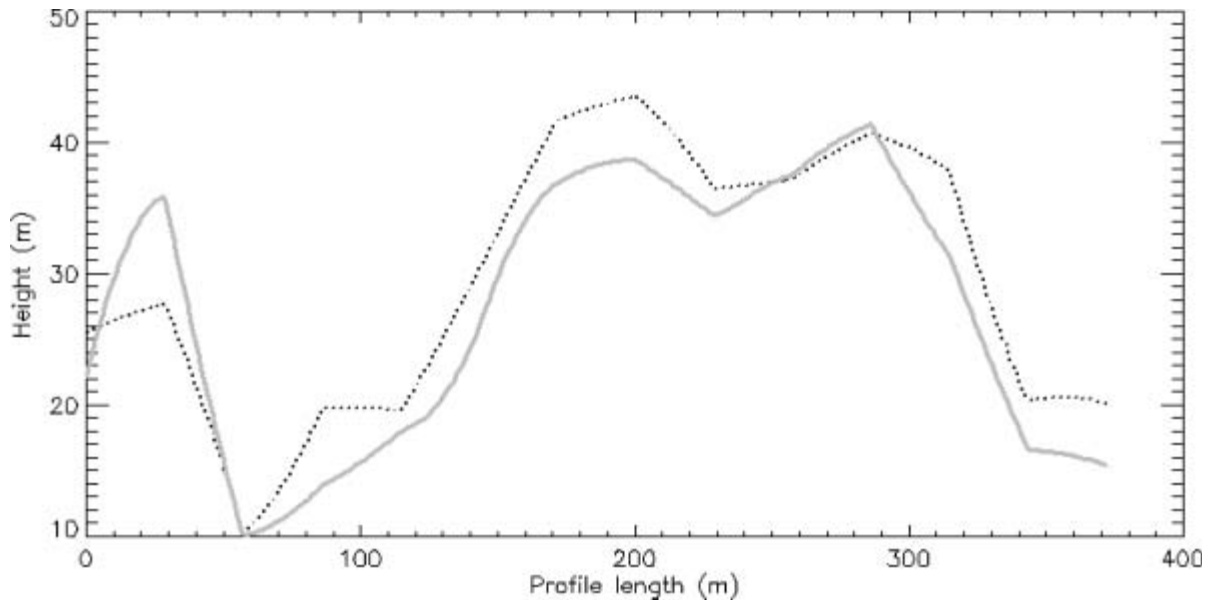


Figure 32. Comparison of maximum height models for IFSAR and LIDAR over length of transect. IFSAR surface shown as solid grey line; LIDAR surface is shown as dotted line.

Conclusions

In a remote sensing context, two basic components are needed to directly characterize vegetation size and density: bare-ground surface elevations and canopy surface elevations. The bare-ground surface provides the point-of-reference needed to compute vegetation heights and to detect the presence or absence of vegetation. Without an accurate bare-ground surface, quantitative information related to plant size and overall vegetation density cannot be derived. Traditional remotely-sensed imagery (LANDSAT, MODIS, SPOT, aerial photographs, and others) can provide information useful for separating different types of vegetation but do not provide direct (as opposed to inferred) measurements necessary to determine the size of individual plants or groups of plants. Two relatively new active remote-sensing tools, interferometric synthetic aperture radar (IFSAR) and light detection and ranging (LIDAR) scanners provide an ability to collect measurements from the ground surface as well as the upper surface of all vegetation visible from the air. However, these new systems are expensive to purchase and operate and generate massive quantities of “raw” data that need extensive processing to provide useful information. The cost of acquiring these data (\$1.00/acre for LIDAR and \$0.10/acre for IFSAR) for large areas remains prohibitive for most forestry applications. However, the basic information products, which are useful within a variety of disciplines, provide the incentive for large-area acquisitions involving entire counties or states. In heavily vegetated areas, IFSAR collected with restricted frequency constraints does not provide sufficiently accurate ground surface models if accurate vegetation heights are to be generated. Fortunately, LIDAR, when acquired and processed correctly, has been shown to provide extremely accurate ground surface models, even in areas of heavy vegetation cover. Given the relatively slow rate of change for the ground surface, a LIDAR bare-ground surface model does not need to be updated frequently. Once such a model is available, it can be used with IFSAR data

to characterize the vegetation at a point in time or changes to vegetation characteristics over time.

Results of the IFSAR P-band ground surface evaluation conducted on the Capitol State Forest in western Washington State, USA study site indicate that airborne P-band IFSAR can be used to provide a bare ground surface when the data are collected without the frequency “notching” required by the FCC. In another acquisition conducted in Columbia, South America, EarthData found that airborne P-band data collected without the frequency restrictions could be processed to provide a reasonable ground surface thus allowing direct measurement of vegetation height. However, given that these frequency restrictions will exist in the United States for the foreseeable future, the usefulness of P-band data is doubtful. When merged with an accurate bare ground surface, whether derived from P-band data or LIDAR, X-band IFSAR provides spatially explicit indicators of the presence or absence of vegetation and a spatially explicit measure of the relative quantity of above ground biomass.

If a suitable bare-ground surface model is available, IFSAR becomes a viable tool for characterizing vegetation size and density. In studies conducted at the Mission Creek, WA site reasonable vegetation heights were derived from X-band IFSAR canopy height model combined with a high-quality LIDAR ground model. This study also helped to show the effect of various acquisition parameters on the overall ability to measure vegetation heights with X-band IFSAR. The results shown in Table 11 indicate that the difference in flying heights studied here has little effect on the accuracy of canopy height measurements. For both of the single flight lines used in this comparison of flying heights, the median error for 90th percentile canopy height measurements was approximately -7m, with a QD of approximately 3 m. The maximum height measurements were also not significantly different at the two different flying heights. This indicates that there would be a minimal gain by acquiring IFSAR at 4,500m versus 6,000m for forest measurement purposes.

Varying the filtering parameters (Table 12) does not appear to have a significant effect on the accuracy of 90th percentile canopy height measurements. The median error is approximately -6m, with a QD of approximately 2.5m at all filtering levels. The level of filtering does have a significant effect on the measurement of maximum height, with higher levels of filtering leading to greater underestimation of maximum canopy height. The magnitude of the median error ranges from -2.5m (QD of 4.4 m) for the filtering level of 1 (no filtering) to -9.9m (QD of 3.6 m) for the highest filtering level.

As expected, using a combination of several overlapping look directions (Table 13) can significantly improve the accuracy of canopy measurements. Due to the shallow look angles characteristic of IFSAR sensing, measurements of forest canopy surface acquired from a single flight line will have many areas where canopy surface features are fully or partially occluded by the topography and localized canopy relief. Although radar shadow areas were excluded from this analysis, it is expected that IFSAR elevation measurements will generally be most accurate in areas where the measurement is obtained from a direct reflection from an unobstructed canopy surface.

Acquiring data from several different directions can help to maximize the IFSAR measurements that represent direct (optimal) measurements of the canopy surface and will therefore improve overall characterization of forest canopy surface structure. The results of this study indicate that using a combination of two different looks will generally provide a significant increase in accuracy over a single look, as the errors of the merged surfaces for all combinations of looks (median errors of -1 to -3m, from Table 13) are lower than that for a single look (median error of -7m, from Table 12). Not surprisingly, the highest quality surface is the result of merging the data from all four looks, with a median error of -0.8m and a QD of 2.0 m. The results indicate that acquiring IFSAR data from multiple look directions is critically important in forestry applications, especially in mountainous areas.

The results seen here provide a confirmation of previous studies: terrain slope will influence the accuracy of IFSAR canopy height estimation when IFSAR is generated from a single pass. Table 14 indicates that the accuracy of the IFSAR canopy height and maximum height measurements obtained from a single pass will decrease with increasing slope. The results also show that using IFSAR canopy models developed from a combination of looks will largely mitigate the effects of slope on the accuracy of canopy measurements. The results in Table 15 indicate that the use of multiple look IFSAR data reduced the underestimation of canopy height at higher slopes (-3.2m median error in canopy height at 0-10° to + 0.5m median error at 40-50°), but there is increased random error in the height measurements as the slope increases (0.8m QD at 0-10° to 2.6m QD at 40-50°). It should be noted that the effects of slope and canopy density are somewhat difficult to separate, as canopy density is certainly influenced by the terrain slope in this area (i.e. low canopy densities on dry ridge crests, high canopy density in moist drainages).

The results of this study also indicate that the accuracy of IFSAR canopy height measurements will be heavily influenced by canopy density (see Table 16). In low density areas, the IFSAR measurements do not capture gaps between the trees, and canopy height represents measurements in the upper portion of the tree crown, while the lidar canopy height is more influenced by canopy openings, leading to an overestimation of generalized canopy height in the IFSAR models (4.9m median error and 2.8m QD in 0-10% CC class). It should be noted that this result runs counter to the findings of Izzawati et al. (2006), where height underestimation increased with decreasing canopy density. This difference in results is most likely due to the use of multiple passes of IFSAR data in our study, but this issue requires further investigation. However, we did find that the discrepancy between the lidar and IFSAR-derived canopy height measurements decreases with increasing canopy density (with a median error of -0.6m and QD of 1.5m for 90-100% CC class), which is consistent with the results of previous studies.

Estimating canopy cover or vegetation density using only IFSAR elevation data is a difficult proposition. In general, the sensing geometry of IFSAR does not allow for accurate measurement of high frequency details in the morphology of the canopy surface, including canopy gaps and smaller individual tree crowns. In the IFSAR canopy

height model, individual tree crowns tend to be smoothed, and canopy gaps are 'filled in' (Figure 30). Therefore, in forests with a relatively discontinuous canopy surface structure and many gaps, a canopy cover or vegetation density estimate derived from the IFSAR canopy height model will tend to be higher than the lidar-based canopy cover estimate. Because of the inability to measure the fine-scale structure of the canopy surface, IFSAR (in contrast to lidar) is unlikely to be used operationally as a forest measurement tool when detailed information is needed for project-level analyses and planning. It is more suited for large-area resource assessment and monitoring applications or for characterizing general vegetation characteristics over large land areas where sufficiently accurate bare-ground models have already been developed using another technique.

Recommendations Regarding the Use of IFSAR Data for Vegetation Mapping

Due to restrictions on use of certain radar frequencies, P-band IFSAR data cannot be reliably used in the United States to obtain bare-ground surfaces. X-band IFSAR produces a surface that poorly represents the ground in areas with vegetation cover. In addition, it does not provide a consistent measure of vegetation height in areas with sparse cover or a mixture of height classes. If a good bare-ground surface is available (perhaps from a LIDAR acquisition), X-band IFSAR data can be used to produce estimates of average canopy height and total above-ground biomass over large land areas. The relatively low cost for acquiring IFSAR data makes it an attractive alternative to both LIDAR and field surveys to obtain biomass and fuel information for large land areas. While the technology exists to use passively sensed images (like the ISTAR images examined in this study) to derive ground surface products and vegetation heights, procedures and current software focus on extracting only bare-ground information, thus, do not currently provide data useful for characterizing vegetation characteristics. The relatively automated procedures used to produce three-dimensional data from such images rely on matching features evident in two or more images covering the same area. Because the ground offers few identifiable features, the objects/image segments used for the matching are often isolated plants. The net result is that the final ground surface is adversely influenced by the vegetation making it difficult to evaluate the ground surface and reducing the overall confidence in vegetation heights derived using the ground surface.

Acknowledgements

We would like to thank the Joint Fire Science Program for funding this study. Special thanks and appreciation go out to graduate students at the University of Washington for their valiant efforts conducting field work in some of the most inhospitable conditions they will ever encounter and their efforts and assistance with data processing and analysis: Andrew Cooke, SooYoung Kim, Akira Kato, Jacob Strunk, Nan Hu, Tobey Clarkin, Yuzhen Lee, and Tracey Marsh. Finally we would like to acknowledge the assistance of several individuals on the San Bernardino and Los Padres National Forest staffs who helped with logistics and access to gated areas during the field seasons of 2004 and 2005. A final thank you to Sean Redar, San Bernardino National Forest, for

help in acquiring and making sense out of a variety of data layers used in the post-fire recovery planning efforts.

Literature Cited

Baltsavias, E.P., 1999, Airborne laser scanning: basic relations and formulas, ISPRS Journal of Photogrammetry and Remote Sensing 54: 199-214.

Carson, W.W., and Reutebuch, S.E. 1997. A rigorous test of the accuracy of USGS digital elevation models in forested areas of Oregon and Washington. In Proceedings of the 1997 ACSM/ASPRS Annual Convention, 7–10 April 1997, Seattle, Wash. American Society for Photogrammetry and Remote Sensing, Bethesda, Md. Vol. 1, pp. 133–143.

Cloude, S.R. and K.P. Papathanassiou. 1998. Polarimetric SAR Interferometry. IEEE Transactions on Geoscience and Remote Sensing 36(4): 1551-1565.

Cooke, Andrew G. 2008. Analysis of LIDAR-derived bare ground model accuracy in southern California chaparral. MS Thesis, University of Washington, Seattle, WA. 123 p.

Curtis, R., Marshall, D., and DeBell, D. (Editors). 2004. Silvicultural options for young-growth Douglas-fir forests: the Capitol Forest study—establishment and first results. US Department of Agriculture Forest Service, Pacific Northwest Research Station, Portland, OR, General Technical Report PNW-GTR-598.

Dutra, L., M. Elmiro, C. Freitas, J.R. Santos, J.C. Mura, and B. Filho, 2002. The use of multi-frequency interferometric products to improve SAR imagery interpretability and classification by image fusion. In: Anais do III Workshop em Tratamento de Imagens, Junho 2002, Belo Horizonte, Minas Gerais, Brazil.

Goodwin, Nicholas R., N.C. Coops, D.S. Culvenor. 2006. Assessment of forest structure with airborne LiDAR and the effects of platform altitude. Remote Sensing of Environment, 103:140-152.

Hagberg, J., L. Ulander, and J. Askne. 1995. Repeat-pass SAR interferometry over forested terrain. IEEE Transactions on Geoscience and Remote Sensing 33(2): 331-340.

Hofmann, C., M. Schwäbisch, S. Och, C. Wimmer, and J. Moreira. Multipath P-band interferometry –first results. Proceedings of the Fourth International Airborne Remote Sensing Conference and Exhibition/21st Canadian Symposium on Remote Sensing. Ottawa, Ontario, Canada, June 21-24, 1999.

Hussin, Y.A., R.M. Reich, and R.M. Hoffer. 1991. Estimating slash pine biomass using radar backscatter. IEEE Transactions on Geoscience and Remote Sensing 29(3):427-431.

Izzawati,, Wallington, E.D. and Woodhouse, I.H., 2006, Forest height retrieval from commercial X-band SAR products. *IEEE Transactions on Geoscience and Remote Sensing*, 44, pp. 863–870.

Kraus, K. and N. Pfeifer. 1998. Determination of terrain models in wooded areas with airborne laser scanner data. *ISPRS Journal of Photogrammetry & Remote Sensing*, 53: 193-203.

Lefsky, M.A., Cohen, W.B., Parker, G.G., and Harding, D.J., 2002, Lidar remote sensing for ecosystem studies, *BioScience* 52: 19-30.

Mercer, B. 2004. DEMs created from airborne IFSAR — an update. *International Archives of Photogrammetry and Remote Sensing*. Vol. 35, part B. CD-ROM.

Mette, T. K. P. Papathanassiou, I. Hajnsek, and R. Zimmermann. Forest biomass estimation using polarimetric SAR interferometry. 2003. *Proceedings of the PolInSAR Conference, Frascati, Italy, Jan. 2003.*

Moreira, J., Schwäbisch, M., Wimmer, C., Rombach, M., and Mura, J., 2001, Surface and ground topography determination in tropical rainforest areas using airborne interferometric SAR, in: *Photogrammetric Week '01'*, Fritsch, D. and R. Spiller, eds. Herbert Wichmann Verlag, Heidelberg.

Mura, J., L. Bins, F. Gama, C. Freitas, J. Santos, and L. Dutra, 2001. Identification of the tropical forest in Brazilian Amazon based on the DEM difference from P- and X-band interferometric data. In: *Proceedings of the Geoscience and Remote Sensing Symposium 2001, IGARSS '01, Sydney, Australia. IEEE, vol. 2. pp. 789-791.*

Reutebuch, Stephen E., R.J. McGaughey, H.E. Andersen, W.W. Carson. 2003. Accuracy of a high-resolution lidar terrain model under a conifer forest canopy. *Canadian Journal of Remote Sensing*, 29(5): 527-535.

Schwäbisch, M. and J. Moreira, 1999. The high resolution airborne interferometric SAR AeS-1. In: *Proceedings of the Fourth International Airborne Remote Sensing Conference and Exhibition/ 21st Canadian Symposium on Remote Sensing, Ottawa, Ontario, Canada.*

Streutker, David R., N.F. Glenn. 2006. LiDAR measurement of sagebrush steppe vegetation heights. *Remote Sensing of Environment*, 102:135-145.

Treuhaft, R.N., S.N. Madsen, M. Moghaddam, and J.J. van Zyl. 1996. Vegetation characteristics and underlying topography from interferometric radar. *Radio Science* 31(6): 1449-1485.

Appendices

Appendix A -- Field Plot Measurement Protocol

Shrub cover is sampled using a 1/25-ha square plot (20- by 20-meter) with 121 (or 36) sample points evenly distributed over the plot. Each sample point represents 4 square meters (2- by 2-meter sample area) or 16 square meters (4- by 4-meter sample area).

The following information is recorded for the plot:

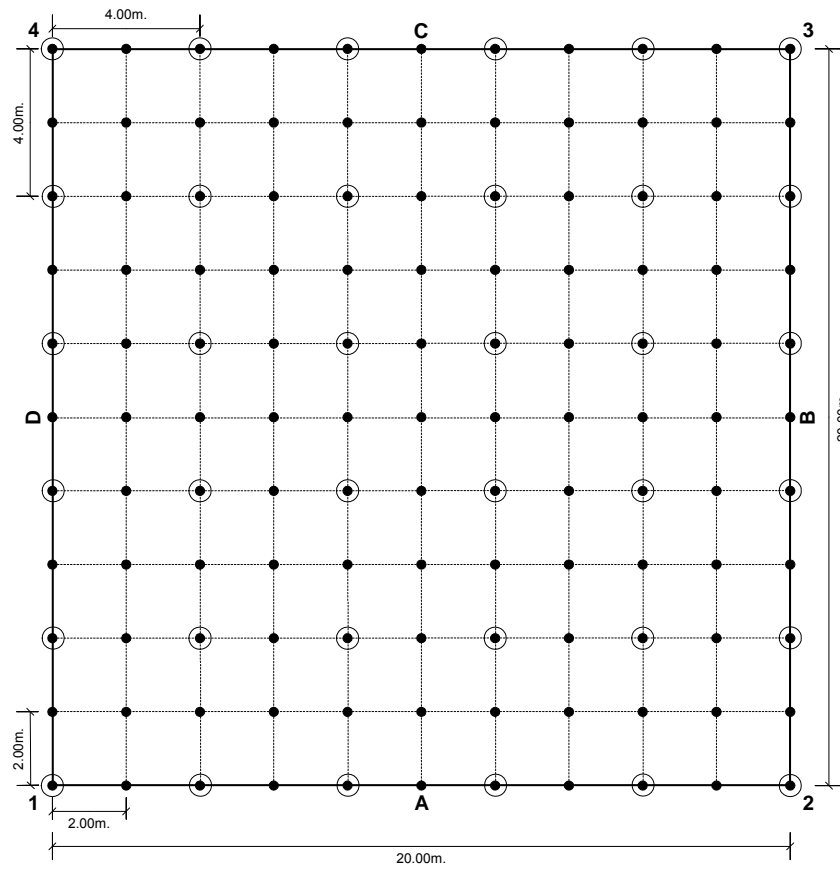
- Plot number,
- Measurement date and time
- Crew members and responsibilities (estimator and recorder),
- General location description (where is the plot, how do you get to the plot),
- General vegetation description (grass, shrub, mixed shrub/small trees),
- Slope, aspect, and elevation at plot center,
- GPS ID of the trilateration points,
- Fore- and back-shots between trilateration points,
- Shots from each trilateration point to the 4 plot corners,
- Photo information,
- Sketch of the plot conditions,
- Comments.

The following information is recorded for each sample point:

- Maximum vegetation height (meters to the nearest 0.1m),
- Height to the base of the foliage layer,
- Dominant species at the point,
- Other species at the point,
- Indicator of whether or not there is vegetation present at 0.5m height intervals. Indicators are recorded starting at the ground (height = 0.0). A "1" is entered if vegetation/foilage is present at the height and a "0" if no vegetation /foilage is present.

Shrub/cover plots can be measured using a 2- by 2-m cell or a 4- by 4-m cell. When the 4- by 4-m cell is used, the height interval for recording structure is 1.0m.

Shrub/cover plots are located using a unique combination of post-processed GPS points and shots taken with IMPULSE measurement instruments. Precise ground positions are established using 3 points and a series of fore-and back-sightings from each of the points to the others. These trilateration points are post processed and a declination angle is computed using a program developed by Ward W. Carson, PNW Research Station. The four plot corners are then shot from each of the trilateration points. This procedure resulted in precise locations for the plot corners. Tree and plant locations for mapped plots are referenced to either the plot corners or one of the trilateration points. All GPS points are collected using a Trimble Pro XL GPS receiver.



Schematic of the shrub plot design

Plot location and layout

Shrub plots should be located within areas of homogeneous vegetation conditions (density and height) and uniform terrain conditions. Plot locations are not randomized and should not include more than one vegetation/structure type. Plots are located starting at corner 1. All four corners are referenced to the trilateration points. The bottom edge of the plot (side A) is oriented so it runs parallel to the ground contour (across the slope). This should make it a little easier to layout and measure the grid transects. Plot corners are temporarily staked with tall poles and later with semi-permanent plastic pegs. General directions from a convenient reference point (recognizable road intersection or other prominent landmark) to the plot are recorded in the *Location description* block of the data sheets. All GPS positions should be computed and recorded in UTM, NAD83. GPS elevations do not need to be recorded. However, GPS elevation is sufficient for the overall plot elevation.

Plots are located and laid out using the following procedure:

- 1 Locate corner 1 of the plot and visually check to make sure the area within the plot exhibits homogeneous vegetation conditions and relatively uniform terrain conditions.
- 2 Drive a tall (10-foot length of EMT) pole at the plot corner (this is a temporary marker).
- 3 Attach three layout ropes to the corner pole.

- 4 Decide on the location of the lower edge (side A) of the plot. It should run across the slope. In general the lower edge should be east of the first point.
- 5 Move to corner point 2, dragging two of the layout ropes attached in step 4. Use the ropes to locate the second corner point.
- 6 Drive a tall (10 foot length of EMT) pole at corner 2 (this is a temporary marker).
- 7 Leave the ends of the layout ropes attached in step 4 at this corner.
- 8 Attach one layout rope to the pole at corner 2.
- 9 Establish the side of the plot by turning a 90-degree angle from the plot baseline (be careful to minimize influence of steel corner pole on compass readings)
- 10 Move to corner 3 dragging the layout rope. Use the layout rope to locate the corner point.
- 11 Drive a tall (10 foot length of EMT) pole at the plot corner (this is a temporary marker).
- 12 Attach the end of the layout rope attached in step 10 to the corner pole.
- 13 Establish the top edge (side C) of the plot by turning a 90-degree angle from the plot side (be careful to minimize influence of steel corner pole on compass readings)
- 14 Move to the approximate location of corner 4 dragging the layout rope.
- 15 Retrieve the layout rope left at the corner 1 and pull it to the corner 4.
- 16 Locate corner 4 at the intersection point of the layout ropes from corners 1 and 3.
- 17 Drive a tall (10 foot length of EMT) pole at the plot corner (this is a temporary marker).
- 18 Attach the two layout ropes to the corner pole;
- 19 Return to corner 1 and prepare for measurement collection.
- 20 Locate plot corner points from each of the 3 trilateration points.

Plot measurements—sample points

Measurements for each plot consist of 121 or 36 sample points arranged in a 2- by 2-meter grid or 4- by 4-meter grid within the plot area. Each sample point represents 4 square meters (2- by 2-meter sample area) or 16 square meters (4- by 4-meter sample area). Sample points are measured using 11 or 6 transects that span the width of the plot. Field personnel should adhere to the plot layout protocol and use the layout ropes to ensure that the sample points are reasonably well located over the plot.

For each sample point, the following measurements are recorded: maximum vegetation height (meters), height to the base of the foliage (meters), dominant species present at the point, other species present at the point, indicators or whether or not vegetation/foliage exists at 0.5m or 1.0m intervals starting from the ground. For sample points with no vegetation, record a maximum vegetation height of 0.0 is recorded. Data sheets are included at the end of appendix A.

All vegetation at the sample point is considered. This includes plants that are not rooted at the point. For example, if a branch from a tall shrub hangs over the plot, it should be considered when characterizing the sample point. In many cases, the tallest vegetation for a sample point may be a single branch from a plant rooted some distance from the point.

Make sure measurements are entered in the correct order. The data sheets are designed to record measurements from left to right for all transects. The correct procedure is to start measuring points at plot corner 1 and work towards corner 2 for the first transect. Then reverse direction and return towards corner 1 for the second transect. The data sheets expect that the odd numbered transects will be measured from left to right and the even-numbered transects from right to left. If you make a mistake and enter data for a transect in the wrong order, there is a box to check on the data sheet to indicate that the transect data needs to be reversed when entered into the database.

Quality assurance procedures

Crews should exercise care when collecting measurements. The field data will be extrapolated to cover potentially large land areas and plot-level measurement errors may result in very large errors when data are extrapolated to the project scale. To characterize the variability related to individual bias and skill at estimating percent cover at various heights, every fifth plot should be measured twice with a different individual making the cover estimates. Plot identifiers for re-measured plots should indicate that the plot is a QA plot (use the same plot number and append “QA”). Record which crew members are responsible for various plot measurement tasks in the *Crew members and responsibilities* block of the data sheet.

Plot photographs

The first photo taken for a plot should be an image of page 1 of the data sheets, showing the plot identifier and other information clearly. Usually you can hold the data sheet at arm’s length and take the picture with the sun behind you.

If possible take digital pictures of the entire plot as seen from a distant viewpoint. Corner poles should be left in place for the photos to indicate the plot location and for relative scale. If you cannot locate a photo point that allows a photo of the entire plot, take a few photos showing the vegetation structure and general height. Try to include something in the image to indicate scale such as a corner post or person. If there are any plant species that cannot be identified, take pictures of the plant or collect samples for later identification. There is a block on the data sheet to record information describing the photographs taken for the plot (exposure number).

Plot sketch

Each plot should be sketched to indicate the location of major vegetation and bare areas. The sketches need not be artistic masterpieces but should give an indication of the vegetation location and the relative proportion of the plot covered by vegetation. Include a North arrow in or around the sketch.

Cleaning up the plot

After collecting measurements for the sample points, the corner poles should be pulled and replaced with plastic pegs. All layout ropes are retrieved and coiled for transport or storage. Corner 1 should be marked with two strips of flagging tied across the top of the brush to form an “X” and a strip tied to the corner peg.

Safety concerns

Field crews will be working in rough, uneven terrain with marginal footing. All crew members should wear sturdy boots that provide ankle support. Hot weather can be expected so crew members should plan to carry extra water in their vehicle and use sunscreen to help prevent sunburns. General hazards include poor footing due to rough terrain, loose soils, and low vegetation; coarse vegetation with some species having thorns or spines; poison oak is common throughout the area (see appendix B for poison oak information); and animal encounters. Animal species that may be encountered include snakes (some venomous), mountain lions, and insects.

Equipment

- Layout ropes (nylon line for a string trimmer, 20m long, marks every 2m, attachment loops at each end) (need 5 for a plot)
- Plot corner poles (10-foot $\frac{3}{4}$ -inch EMT, flagging streamers at top, white stripes every $\frac{1}{2}$ meter) (need 4 for a plot)
- Flexible poles for “threading layout ropes under vegetation” or positioning layout ropes on top of vegetation (10-foot $\frac{3}{4}$ ” schedule 40 pipe, capped at both ends, eyebolts installed in caps)
- Ropes to stabilize plot corner poles (15-feet long with loops at each end). These attach to the top of the poles using a wooden dowel that slips inside the EMT pole.
- Plastic stakes for permanent plot corner markers
- Flagging
- Height poles
- GPS unit
- Data sheets
- Clipboard

Calculations

Shrub plot measurements yield the following metrics for the plot: vegetation surface model using the maximum vegetation height measured at each sample point, overall percent cover, percent cover at 1/2m height intervals.

Vegetation surface model

Surface models are created using all maximum vegetation heights for the sample points. Geo-referencing is accomplished using the GPS coordinates for the plot corners and the transect geometry. When building a surface model, all sample points are assumed to be “perfectly” located at the center of the sample area.

Percent cover

Percent cover is computed using the sample point measurements of vegetation height. Overall percent cover is simply the number of points with a non-zero vegetation height divided by 121. Percent cover at a given height is the number of points with vegetation at or below the desired height divided by 121. Percent cover by species is computed using the number of points with the desired species divided by 121. Other cover calculations are possible depending on the analysis methods used to relate the field plots with IFSAR data metrics.

Plot Location Data Sheet

Plot	Date	Time	Crew
Location			
General description			
Vegetation type			
Slope	Aspect	Elevation	

Trilateration points				GPS			Trilateration results		
Point	ID	Easting	Northing	Elevation	Easting	Northing	Elevation	Declination	
1	gps1								
2	gps2								
3	gps3								
4	gps4								

	Horz dist	Azimuth	Vert dist	Prism ht	Laser ht	Adj VD
1 to 2						0.00
1 to 3						0.00
2 to 1						0.00
2 to 3						0.00
3 to 1						0.00
3 to 2						0.00
1 to 4						0.00
2 to 4						0.00
3 to 4						0.00
4 to 1						0.00
4 to 2						0.00
4 to 3						0.00

All coordinate values are UTM meters WGS84
Distances are meters
Angles are azimuth in degrees
Tree diameters in centimeters
Elevations in meters

Plot corners											
From (ID)	To (ID)	Horiz dist	Azimuth	Vert dist	Prism ht	Laser ht	Adj VD	Easting	Northing	Elevation	
1:	c1:						0.00	0.00	0.00	0.00	
1:	c2:						0.00	0.00	0.00	0.00	
1:	c3:						0.00	0.00	0.00	0.00	
1:	c4:						0.00	0.00	0.00	0.00	
2:	c1:						0.00	0.00	0.00	0.00	
2:	c2:						0.00	0.00	0.00	0.00	
2:	c3:						0.00	0.00	0.00	0.00	
2:	c4:						0.00	0.00	0.00	0.00	
3:	c1:						0.00	0.00	0.00	0.00	
3:	c2:						0.00	0.00	0.00	0.00	
3:	c3:						0.00	0.00	0.00	0.00	
3:	c4:						0.00	0.00	0.00	0.00	
4:	c1:						0.00	0.00	0.00	0.00	
4:	c2:						0.00	0.00	0.00	0.00	
4:	c3:						0.00	0.00	0.00	0.00	
4:	c4:						0.00	0.00	0.00	0.00	

Final plot corner locations			
	Easting	Northing	Elevation
c1	0.00	0.00	0.00
c2	0.00	0.00	0.00
c3	0.00	0.00	0.00
c4	0.00	0.00	0.00

Photos

Comments

Plot diagram: Sketch plot with major vegetation features. Include individual plants, clumps, bare areas, and north arrow

Vegetation Grid Data Sheet

Plot	<input type="text"/>	Date	<input type="text"/>	Location	<input type="text"/>	Grid size (2 or 4)	<input type="text"/>
------	----------------------	------	----------------------	----------	----------------------	--------------------	----------------------

Transect 1		pt 1	pt 2	pt 3	pt 4	pt 5	pt 6	pt 7	pt 8	pt 9	pt 10	pt 11
Max veg ht												
Ht to crown base												
Structure	Dominant species											
interval	Other species											
<input type="text"/>	Structure											

Transect 2		pt 1	pt 2	pt 3	pt 4	pt 5	pt 6	pt 7	pt 8	pt 9	pt 10	pt 11
Max veg ht												
Ht to crown base												
Structure	Dominant species											
interval	Other species											
<input type="text"/>	Structure											

Transect 3		pt 1	pt 2	pt 3	pt 4	pt 5	pt 6	pt 7	pt 8	pt 9	pt 10	pt 11
Max veg ht												
Ht to crown base												
Structure	Dominant species											
interval	Other species											
<input type="text"/>	Structure											

Transect 4		pt 1	pt 2	pt 3	pt 4	pt 5	pt 6	pt 7	pt 8	pt 9	pt 10	pt 11
Max veg ht												
Ht to crown base												
Structure	Dominant species											
interval	Other species											
<input type="text"/>	Structure											

Transect 5		pt 1	pt 2	pt 3	pt 4	pt 5	pt 6	pt 7	pt 8	pt 9	pt 10	pt 11
Max veg ht												
Ht to crown base												
Structure	Dominant species											
interval	Other species											
<input type="text"/>	Structure											

Transect 6		pt 1	pt 2	pt 3	pt 4	pt 5	pt 6	pt 7	pt 8	pt 9	pt 10	pt 11
Max veg ht												
Ht to crown base												
Structure	Dominant species											
interval	Other species											
<input type="text"/>	Structure											

Transect 7		pt 1	pt 2	pt 3	pt 4	pt 5	pt 6	pt 7	pt 8	pt 9	pt 10	pt 11
Max veg ht												
Ht to crown base												
Structure	Dominant species											
interval	Other species											
<input type="text"/>	Structure											

Transect 8		pt 1	pt 2	pt 3	pt 4	pt 5	pt 6	pt 7	pt 8	pt 9	pt 10	pt 11
Max veg ht												
Ht to crown base												
Structure	Dominant species											
interval	Other species											
<input type="text"/>	Structure											

Transect 9		pt 1	pt 2	pt 3	pt 4	pt 5	pt 6	pt 7	pt 8	pt 9	pt 10	pt 11
Max veg ht												
Ht to crown base												
Structure	Dominant species											
interval	Other species											
<input type="text"/>	Structure											

Transect 10		pt 1	pt 2	pt 3	pt 4	pt 5	pt 6	pt 7	pt 8	pt 9	pt 10	pt 11
Max veg ht												
Ht to crown base												
Structure	Dominant species											
interval	Other species											
<input type="text"/>	Structure											

Transect 11		pt 1	pt 2	pt 3	pt 4	pt 5	pt 6	pt 7	pt 8	pt 9	pt 10	pt 11
Max veg ht												
Ht to crown base												
Structure	Dominant species											
interval	Other species											
<input type="text"/>	Structure											

Appendix B -- Outputs

Published Outputs

Peer-reviewed journal articles

Andersen, H.-E., R.J. McGaughey, and S.E. Reutebuch. 2008. Assessing the influence of flight parameters, interferometric processing, slope, and canopy density on the accuracy of X-band IFSAR-derived forest canopy height models. *International Journal of Remote Sensing* 29(5): 1495-1510.

Andersen, H.-E., S.E. Reutebuch, and R.J. McGaughey. 2005. Accuracy of an IFSAR-derived digital terrain model under a conifer forest canopy. *Canadian Journal of Remote Sensing* 31(4):283-288.

Peer-reviewed book chapter

Andersen, H.-E., S.E. Reutebuch, and R.J. McGaughey. 2006. Chapter 3: Active remote sensing. In: Shao, G., and K. Reynolds, eds., *Computer Applications in Sustainable Forest Management*, Springer-Verlag, Dordrecht.

Peer-reviewed conference proceedings

Andersen, H.-E., R.J. McGaughey, W.W. Carson, S.E. Reutebuch, B. Mercer, and J. Allan. 2003. A comparison of forest canopy models derived from LIDAR and IFSAR data in a Pacific Northwest conifer forest. *International Archives of Photogrammetry and Remote Sensing*, Dresden, Germany, Vol. XXXIV, Part 3 / W13.

Non-peer-reviewed conference proceedings and technical reports

Andersen, H.-E., S.E. Reutebuch, and R.J. McGaughey. 2006. Assessing the influence of flight parameters and interferometric processing on the accuracy of X-band IFSAR-derived forest canopy surface models. In: Koukal, T. and W. Schneider, eds., *Proceedings of the EARSeL Workshop on 3D Remote Sensing in Forestry, Vienna, Austria, February 14-15, 2006*. University of Natural Resources and Applied Life Sciences (BOKU) Vienna.

Andersen, H.-E., R.J. McGaughey, S.E. Reutebuch, G.F. Schreuder, J. Agee, and B. Mercer. 2004. Estimating canopy fuel parameters in a Pacific Northwest conifer forest using multifrequency polarimetric IFSAR. *International Archives of Photogrammetry and Remote Sensing*, Istanbul, Turkey, Vol. XXXV, Part B.

Dissertation and Theses

Cooke, Andrew G. 2008. Analysis of LIDAR-derived bare ground model accuracy in southern California chaparral. MS Thesis, University of Washington, Seattle, WA. 123 p.

Presentations

Andersen, H.-E. and R.J. McGaughey. 2007. A method to generate detailed forest canopy surface models through the fusion of high-resolution X-band radar backscatter and interferometric height data. *Presentation at the Alaska Surveying and Mapping Conference, Fairbanks, AK, March 19-23, 2007.*

Andersen, H.-E., S.E. Reutebuch, and R.J. McGaughey. 2006. Assessing the influence of flight parameters and interferometric processing on the accuracy of X-band IFSAR-derived forest canopy surface models. *EARSel Workshop on 3D Remote Sensing in Forestry, Vienna, Austria, February 14-15, 2006.*

Andersen, H.-E. 2005. Using high-density LIDAR data to inform the analysis of interferometric phase error and accuracy assessment of InSAR elevation measurements in a forested area. *ISPRS WG1/2 Workshop on 3D Mapping from InSAR and LIDAR, Banff, Canada, June 7-10, 2005.*

Andersen, H.-E., R.J. McGaughey, and S.E. Reutebuch. 2005. The use of high-resolution, active airborne remote sensing technologies to support precision forestry. *Second Appalachian Remote Sensing Conference, West Virginia University, Morgantown, West Virginia, May 11, 2005.* Invited keynote speaker.

Andersen, H.-E., G.F. Schreuder, R.J. McGaughey, S.E. Reutebuch, and W.W. Carson. 2004. Estimating forest inventory parameters using high-resolution LIDAR and IFSAR. *1st International Workshop on Digital Forestry, Beijing, China, June 14-18, 2004.* Invited speaker.